Western University
Scholarship@Western

Paediatrics Publications | Paediatrics Department

1-1-2013

Polysialylated NCAM and EphrinA/EphA regulate synaptic development of gabaergic interneurons in prefrontal cortex

Leann H. Brennaman
UNC School of Medicine

Xuying Zhang
UNC School of Medicine

Hanjun Guan
UNC School of Medicine

Jason W. Triplett
University of California, Santa Cruz

Arthur Brown
Western University, abrown@robarts.ca

See next page for additional authors

Follow this and additional works at: https://ir.lib.uwo.ca/paedpub

Citation of this paper:
Brennaman, Leann H.; Zhang, Xuying; Guan, Hanjun; Triplett, Jason W.; Brown, Arthur; Demyanenko, Galina P.; Manis, Paul B.; Landmesser, Lynn; and Maness, Patricia F., "Polysialylated NCAM and EphrinA/EphA regulate synaptic development of gabaergic interneurons in prefrontal cortex" (2013). *Paediatrics Publications*. 855.
https://ir.lib.uwo.ca/paedpub/855

Authors

Leann H. Brennaman, Xuying Zhang, Hanjun Guan, Jason W. Triplett, Arthur Brown, Galina P. Demyanenko, Paul B. Manis, Lynn Landmesser, and Patricia F. Maness

This article is available at Scholarship@Western: https://ir.lib.uwo.ca/paedpub/855

Cerebral Cortex January 2013;23:162–177
doi:10.1093/cercor/bhr392
Advance Access publication January 23, 2012

Polysialylated NCAM and EphrinA/EphA Regulate Synaptic Development of GABAergic Interneurons in Prefrontal Cortex

Leann H. Brennaman[1], Xuying Zhang[1], Hanjun Guan[1,7], Jason W. Triplett[2,8], Arthur Brown[3], Galina P. Demyanenko[1], Paul B. Manis[4,5], Lynn Landmesser[6] and Patricia F. Maness[1]

[1]Department of Biochemistry and Biophysics, University of North Carolina School of Medicine, Chapel Hill, NC 27599, USA[2]Department of Molecular Cell and Developmental Biology, University of California Santa Cruz, Santa Cruz, CA 95064, USA[3]Department of Anatomy and Cell Biology, University of Western Ontario, Ontario N6A 5C1, Canada[4]Departments of Otolaryngology/Head and Neck Surgery and[5]Cell and Molecular Physiology University of North Carolina School of Medicine, Chapel Hill, NC 27599, USA and[6]Department of Neurosciences Case Western Reserve University, Cleveland, OH 44106, USA

[7]Current address: Department of Biochemistry, University of Kentucky, Lexington, KY 40536, USA
[8]Current address: Center for Neuroscience Research, Children's National Medical Center, Washington, DC 20010, USA

Address correspondence to Dr Patricia F. Maness, Department of Biochemistry and Biophysics, University of North Carolina, 120 Mason Farm Rd., CB# 7260, Chapel Hill, NC 27599, USA. Email: srclab@med.unc.edu.

Downloaded from https://academic.oup.com/cercor/article/23/1/162/331609 by guest on 08 August 2022

A novel function for the neural cell adhesion molecule (NCAM) was identified in ephrinA/EphA-mediated repulsion as an important regulatory mechanism for development of GABAergic inhibitory synaptic connections in mouse prefrontal cortex. Deletion of NCAM, EphA3, or ephrinA2/3/5 in null mutant mice increased the numbers and size of perisomatic synapses between GABAergic basket interneurons and pyramidal cells in the developing cingulate cortex (layers II/III). A functional consequence of NCAM loss was increased amplitudes and faster kinetics of miniature inhibitory postsynaptic currents in NCAM null cingulate cortex. NCAM and EphA3 formed a molecular complex and colocalized with the inhibitory presynaptic marker vesicular GABA transporter (VGAT) in perisomatic puncta and neuropil in the cingulate cortex. EphrinA5 treatment promoted axon remodeling of enhanced green fluorescent protein–labeled basket interneurons in cortical slice cultures and induced growth cone collapse in wild-type but not NCAM null mutant neurons. NCAM modified with polysialic acid (PSA) was required to promote ephrinA5-induced axon remodeling of basket interneurons in cortical slices, likely by providing a permissive environment for ephrinA5/EphA3 signaling. These results reveal a new mechanism in which NCAM and ephrinAs/EphA3 coordinate to constrain GABAergic interneuronal arborization and perisomatic innervation, potentially contributing to excitatory/inhibitory balance in prefrontal cortical circuitry.

Keywords: interneuron, perisomatic innervation, prefrontal cortex, synaptic development

Introduction

Neural cell adhesion molecule (NCAM) is a pivotal regulator of axon growth, fasciculation, and cell adhesion (Maness and Schachner 2007). Mutation or altered expression of NCAM has been linked with schizophrenia (Vawter 2000; Sullivan et al. 2007), bipolar disorder (Atz et al. 2007), and Alzheimer's disease (Santuccione et al. 2005; Aisa et al. 2010). NCAM null mutant mice, which lack the 3 principal NCAM isoforms (NCAM180, 140, and 120), display impaired learning, memory (Cremer et al. 1994; Stork et al. 2000; Montag-Sallaz et al. 2003; Senkov et al. 2006; Jurgenson et al. 2010), and hippocampal long-term potentiation (LTP) (Cremer et al. 1998; Bukalo et al. 2004; Stoenica et al. 2006; Dityatev et al. 2008). In schizophrenia subpopulations, polymorphisms in the NCAM1 gene are specifically associated with cognitive deficits, including defects in working memory, a prefrontal cortical function (Atz et al. 2007; Sullivan et al. 2007). A proteolytic fragment of NCAM consisting of its entire extracellular region (NCAM-EC) is overexpressed in the brain in schizophrenia (van Kammen et al. 1998; Vawter 2000; Vawter et al. 2001) but is also present at low levels in normal brain development (Brennaman and Maness 2008; Cox et al. 2009). The NCAM-EC fragment is generated by cleavage of transmembrane isoforms by the ADAM (a disintegrin and metalloprotease) family proteases, ADAM10 (Hinkle et al. 2006) and ADAM17 (Kalus et al. 2006). The NCAM extracellular region is also subject to polysialylation (PSA-NCAM), which is important for synaptic plasticity (Rutishauser 2008). PSA-NCAM is a highly glycosylated form of NCAM that is abundant in embryonic and early development and presents at lower levels in adult brain (Bonfanti 2006; Gascon et al. 2007; Rutishauser 2008). PSA-NCAM is reduced in schizophrenia within the hippocampus (Barbeau et al. 1995), and polymorphisms in the genetic locus of ST8SiaII/STX, a sialyltransferase that polysialylates NCAM (Weinhold et al. 2005), are associated with schizophrenia (Arai et al. 2006; Tao et al. 2007; Isomura et al. 2011), autism (Anney et al. 2010), and bipolar disorder (Lee et al. 2011).

Transgenic mice that overexpress the NCAM-EC fragment in cortical neurons (Pillai-Nair et al. 2005) display reduced connectivity of GABAergic inhibitory neurons in the prefrontal cortex (PFC), accompanied by deficits in sensory gating, emotional memory, locomotion (Pillai-Nair et al. 2005), working memory, and LTP (Brennaman et al. 2011). Strikingly, axon arbors of parvalbumin-positive basket interneurons are diminished in the NCAM-EC transgenic cingulate cortex, and perisomatic innervation of pyramidal cell soma is reduced (Pillai-Nair et al. 2005; Brennaman and Maness 2008). Basket cell axons normally arborize profusely and form synaptic puncta on the soma and proximal dendrites of multiple pyramidal cells (Freund and Katona 2007) to regulate synchronous firing (Klausberger et al. 2003; Sohal et al. 2009) important for working memory (Whittington and Traub 2003).

Based on the involvement of NCAM in learning and memory and the effect of NCAM-EC overexpression on basket interneuron connectivity, we reasoned that NCAM might contribute to cortical excitatory–inhibitory balance by regulating basket cell arborization and synaptogenesis. EphA3 has been implicated as a potential risk gene in autism (Casey et al.

© The Author 2012. Published by Oxford University Press. All rights reserved.
For permissions, please e-mail: journals.permissions@oup.com

2011), and PSA-NCAM has been shown to cooperate with EphAs to regulate hippocampal mossy fiber terminal arborization (Galimberti et al. 2010). However, a potential interaction between NCAM and ephrinA/EphA in regulating cortical interneuron connectivity has not been investigated.

Here, we report that NCAM cooperates with the ephrinA/EphA system to constrain arborization of GABAergic interneurons and to limit functional perisomatic synapse formation in the mouse PFC. The interaction of NCAM with the ephrinA/EphA system may serve to regulate the balance of excitation and inhibition in the developing PFC.

Materials and Methods

Mice

NCAM null mutant (Cremer et al. 1994; Hata et al. 2007), EphA3 null (Vaidya et al. 2003), ephrinA3 null, ephrinA5 null (Cutforth et al. 2003), ephrinA2/3/5 triple null (Pfeiffenberger et al. 2005), bacterial artificial chromosome (BAC) transgenic GAD67–enhanced green fluorescent protein (EGFP) (Chattopadhyaya et al. 2004), and wild-type (WT) (C57Bl/6 or 129) mice of both genders were used for these studies. Embryonic day 0.5 (E0.5) was defined as the plug date, and the day of birth as postnatal day 0 (P0). All animals were used according to the University of North Carolina Institutional Animal Care and Use Committee policies and in accordance with National Institutes of Health guidelines.

Immunochemicals and Reagents

Polyclonal antibodies (pAbs) were used against EphA3 (C-19 and L-18), EphA4 (S-20), NCAM (H300), Neurexin 1 (P-15), Neuroligin 2 (R-16) (Santa Cruz Biotechnology), EphA4 (Zymed), γ-aminobutyric acid (GABA; Sigma), GABA transporter 1 (GAT-1), NCAM Ab5032 (Millipore), ephrinA5 (Abcam, ab70114), vesicular GABA transporter (VGAT; Synaptic Systems), and EphA7 (R&D Systems; AF608). Monoclonal antibodies (mAbs) used were directed to common determinants in the NCAM180/140 cytoplasmic domain (clone OB11, Sigma-Aldrich; or clone AG1, Developmental Studies Hybridoma Bank, University of Iowa), parvalbumin (Sigma-Aldrich), glutamic acid decarboxylase-65 kDa (GAD65), NeuN (Millipore), gephyrin, VGAT (Synaptic Systems), and PSA (5A5, gift of Urs Rutishauser; MAB5234, Millipore). The GAD65 antibody recognizes only the GAD65 and its 2 degradation products and not GAD67 (Chang and Gottlieb 1988; Essrich et al. 1998). Other antibodies included AlexaFluor-488–conjugated anti-GFP (Molecular Probes), secondary antibodies, and normal human, rabbit, and mouse IgG (Jackson ImmunoResearch Laboratories). EphrinA5 fused to alkaline phosphatase (ephrinA5-AP) was generated from an expression plasmid (Ciossek et al. 1998; Schlatter et al. 2008). Note that ephrinA5-Fc and ephrinA5-AP produce similar results in culture and are interchangeable. Other proteins included purified AP (Roche), rhodamine-conjugated phalloidin (Molecular Probes), and ephrinA5-Fc (R&D Systems). NCAM-Fc fusion protein was produced as described (Meiri et al. 1998). Endoneuraminidase-N (endo-N), which removes α-2,8 sialic acid chains, was a gift of Urs Rutishauser (El Maarouf and Rutishauser 2003).

Immunofluorescence Staining

Mice were anesthetized, perfused transcardially with 4% paraformaldehyde (PFA), and processed for staining as described (Demyanenko et al. 1999). Brains were removed and postfixed in 4% PFA overnight at 4 °C, cryoprotected in a 10–30% sucrose series, and cryosectioned (16 μm). Sections were permeabilized in 1% NonidetP-40 (NP-40) and blocked in 5% normal donkey serum/5% nonfat dry milk in phosphate buffered saline (PBS) for 1 h at room temperature. Sections were incubated with antibodies against EphA3 (C-19, 1:50), NCAM AG1 (1:100), NCAM Ab5032 (1:200), PSA (5A5, 1:1000), gephyrin (1:200), VGAT (1:500), parvalbumin (1:500), GAD65 (1:40), or AlexaFluor-488–conjugated anti-GFP (1:200) overnight at 4 °C in 1% normal donkey serum/PBS, then with Cy5-labeled (1:150), AlexaFluor-488–labeled, or AlexaFluor-546–labeled secondary antibodies (1:400) for 1 h at room temperature, mounted in Vectashield, and images captured on an Olympus FV500 confocal microscope using a ×60 objective with ×2.5 optical zoom in the UNC Microscopy Services Laboratory (Dr Robert Bagnell, Director).

Whole-Cell Patch-Clamp Recordings

Mice were anesthetized with ketamine (80 mg/kg)—xylazine (8 mg/kg) and decapitated. Coronal slices (350 μm) of the anterior cingulate cortex were prepared from P21–P27 WT and NCAM null mutant mice in ice-cold oxygenated high-sucrose artificial cerebrospinal fluid (240 mM sucrose, 26 mM $NaHCO_3$, 2.5 mM KCl, 1 mM $CaCl_2$, 4 mM $MgSO_4$, 1.25 mM NaH_2PO_4, 10 mM D-glucose; pH 7.4; gassed with 95% O_2/5% CO_2). The slices were then incubated in extracellular recording solution (125 mM NaCl, 2.5 mM KCl, 2 mM $CaCl_2$, 1.3 mM $MgSO_4$, 20 mM D-glucose, 1.25 mM NaH_2PO_4, 26 mM $NaHCO_3$; pH 7.4; gassed with 95% O_2/5% CO_2) for 30 min at 34 °C, followed by at least 30 min at room temperature. Miniature inhibitory postsynaptic current (mIPSC) was recorded from pyramidal cells of layer II/III of the anterior cingulate cortex. Pyramidal neurons were voltage clamped in whole-cell mode with a recording pipette containing 68 mM $CsMetSO_3$, 72 mM CsCl, 5 mM ethylene glycol tetraacetic acid (EGTA), 10 mM 4-(2-hydroxyethyl)-1-piperazineethanesulfonic acid (HEPES), 4 mM adenosine triphosphate, 0.3 mM guanosine triphosphate, 10 mM creatine phosphate, and 3 mM QX 314 chloride. AlexaFluor 488 (0.1%, w/v; Invitrogen) was added to the internal solution to provide morphological identification of all recorded cells, and only pyramidal neurons were studied. To isolate GABAergic mIPSCs, the extracellular solution was supplemented with 1 μM tetrodotoxin to block action potentials, 10 μM 6-cyano-7-nitroquinoxaline-2,3-dione (CNQX) to block AMPA-mediated transmission, and 50 μM 2,5-aminophosphonovalerate (AP5) to inhibit NMDA-dependent currents. No compensation was used. All chemicals were obtained from Sigma-Aldrich, except CNQX and AP5, which were purchased from Tocris Bioscience. Recordings were made with an AxoClamp 700B Amplifier (Molecular Devices) and acquired with a custom MATLAB program (R2011a; The Mathworks). All recordings were made at 34 °C. Data were analyzed by MATLAB, Igor Pro (6.21; Wavemetrics) and by MiniAnalysis (Synaptsoft, Inc.). mIPSC was recorded from 10 to 12 neurons per genotype (P21–P27 littermates; WT $n = 4$ mice, NCAM null $n = 5$ mice).

In Situ Hybridization

Digoxigenin-labeled riboprobes (sense and antisense) for ephrinA5 were generated by in vitro transcription from pBlueScript (SK) plasmids containing mouse ephrinA5 complementary deoxyribonucleic acid (cDNA) (gift of David Feldheim). WT mice (P15) were perfused transcardially with 4% PFA, brains were removed, immersion fixed in 4% PFA overnight, and cryoprotected in sucrose before sectioning sagittally. In situ hybridization (ISH) was performed as described (Colbert et al. 1995) in the histology core facility of the Neuroscience Center at the University of North Carolina-Chapel Hill, and images were captured digitally on a Zeiss Axioplan 2 microscope.

Cortical Slice Cultures

Organotypic slice cultures were prepared by sectioning the cingulate cortex of WT or NCAM null GAD67-EGFP mice (P5) in the coronal plane (400 μm). Slices were cultured in Dulbecco's Modified Eagle's Media (DMEM)-containing 20% horse serum, 1 mM glutamine, 13 mM glucose, 1 mM $CaCl_2$, 2 mM $MgSO_4$, 0.5 μm/mL insulin, 30 mM HEPES, 5 mM $NaHCO_3$, and 0.001% ascorbic acid, which was replaced every 2 days, as described (Chattopadhyaya et al. 2004). In some experiments, slices at 8 days in vitro (DIV) were treated with ephrinA5-AP (5 μg/mL) or AP every other day until 14 DIV, while in others, ephrinA5-AP or AP treatment occurred for 1 h on slices at 14 DIV. For experiments where slices were treated with endo-N, slices were treated at 6 DIV with 20 U of endo-N (El Maarouf and Rutishauser 2003). Slices were fixed in 4% PFA and stained with antibodies to NeuN to mark neuronal nuclei (Kim et al. 2009; 1:400) or PSA (5A5; 1:1000) followed by Tetramethyl

Downloaded from https://academic.oup.com/cercor/article/23/1/162/331609 by guest on 08 August 2022

Rhodamine Iso-Thiocyanate-labeled anti-mouse secondary antibody (1:150) and AlexaFluor-488–conjugated anti-GFP antibodies (1:400).

Analysis of Perisomatic Innervation, Process Growth, and Branching of Interneurons

EGFP-labeled basket interneurons in layers II/III of anterior cingulate slice cultures were fully imaged in a *z*-series (0.5–1 μm steps; 30–60 sections per *z*-stack) on an Olympus FV500 confocal microscope (×20, ×1 optical zoom) in the UNC Microscopy Services Laboratory, and the entire arbor of each basket cell was reconstructed using Neurolucida software as described (Brennaman and Maness 2008). Similar analyses were performed on slice cultures from WT and NCAM null mice treated with AP or ephrinA5-AP for 1 h or 6 days (5 μg/mL) with and without endo-N treatment. Dendrites and axons of basket interneurons are not readily distinguishable in rodent frontal cortex because the dendrites bear few spines (Hartwich et al. 2009); hence, all processes were considered as a group. Data analysis was automated using MATLAB software. Statistical significance was assessed using two-factor analysis of variance (ANOVA) ($P < 0.05$).

To quantify perisomatic synaptic puncta, single optical sections (Olympus FV500 confocal microscope, ×60, ×1 optical zoom) were analyzed for GFP-labeled puncta surrounding NeuN-labeled somata within 2 μm of the nucleus. In each case, 3–5 slices per mouse ($n = 3$–5 animals/genotype) per condition or time point were scored for perisomatic innervation, neurite growth, and branching. The mean number of perisomatic synaptic puncta was quantified by counting the number of fluorescent puncta for 5–10 somata. In some sections, processes would cross over NeuN-positive soma. Processes contacting a soma without evidence of puncta formation were not scored as these were determined to be dendrites as there was no difference in the number of these processes when comparing conditions. The area of individual synaptic puncta was determined using ImageJ software by outlining 5 randomly selected perisomatic puncta on each of 5 pyramidal cells per image. Neurons (100–200) per genotype were scored for puncta number and area to determine mean values. Student's *t*-test was applied to evaluate significant mean differences ($P < 0.05$).

Interneuron densities in layer II/III of the cingulate cortex were determined by scoring cells under fluorescence microscopy within a unit area of 5–8 serial coronal sections from WT, NCAM-, EphA3-, or ephrinA-null mice ($n = 3$ per genotype) after immunostaining with parvalbumin mAb (1:500). The unit area of layer II/III of the cingulate cortex was determined for each section using ImageJ software, and only parvalbumin-positive interneurons located within this boundary were counted. Neuron counts were represented as number of cells per square millimeter.

Growth Cone Collapse Assay

Dissociated cortical neuron cultures (~80% pyramidal neurons, ~20% interneurons; Waagepetersen et al. 2002) were generated from P0 mice (Hinkle et al. 2006; Brennaman and Maness 2008) and cultured as described (Wright et al. 2007; Schlatter et al. 2008). After 48 h, ephrinA5-Fc or human IgG (3 μg/mL) was added for 30 min. Neurons were fixed and growth cones visualized by immunofluorescence for phalloidin (Wright et al. 2007; Schlatter et al. 2008), followed by labeling with anti-GABA antibodies (1:200). Growth cones were scored as collapsed versus noncollapsed by a bullet-shaped morphology as compared with a spread morphology, respectively, by established criteria (Cox et al. 1990). Growth cone collapse was expressed as the percentage of neurons with collapsed growth cones (10 fields per well; ⩾2 wells per experiment; ⩾300 growth cones). GABA-positive and GABA-negative neurons were scored separately. At least 300 growth cones were scored per condition ($n = 3$–5 mice) for each experiment.

Immunoprecipitations and Pull-Down Assays

Proteins from cell lysates or brain extracts (1 mg) in radio immunoprecipitation assay buffer (20 mM Tris pH 7.0, 0.15 M NaCl, 5 mM ethylenediaminetetraacetic acid, 1 mM EGTA, 1% NP-40, 1% deoxycholate, 0.1% sodium dodecyl sulfate (SDS), 200 μm Na_3VO_4, 10 mM NaF, 1X protease inhibitors [Sigma]) were produced as described (Hinkle et al. 2006) and precipitated using antibodies against EphA3 (C-19 and L-18 pAbs), EphA4 (Santa Cruz), EphA7, Neurexin 1 or Neuroligin 2, and protein A/G agarose beads (ThermoFisher). In some experiments, brain extracts were treated for 1 h with endo-N (40 U) on ice prior to immunoprecipitation to remove PSA. For coimmunoprecipitation of EphA3 and NCAM140, HEK293T cells (DMEM, 5% fetal bovine serum) were transfected with EphA3 and NCAM140 cDNA using Lipofectamine 2000 (Invitrogen) according to the manufacturer's instructions. For the pull-down assays, HEK293T cells were transfected with EphA3, NCAM140, or NCAM180 cDNAs. After 48 h, proteins from cell lysates (500 μg) were incubated with ephrinA5-Fc or NCAM-Fc proteins and protein A/G agarose beads to detect protein interactions. Normal rabbit IgG (nIg) was used as a control. Protein complexes were separated by SDS-polyacrylamide gel electrophoresis and immunoblotted using antibodies to ephrinA5, EphA3, EphA4, EphA7, NCAM (extracellular and intracellular domains), PSA (MAB5234), Neurexin 1, or Neuroligin 2.

Results

Increased Perisomatic Synapses of GABAergic Interneurons in the Cingulate Cortex of NCAM Null Mutant Mice Results in Enhanced Inhibitory Neurotransmission

Perisomatic inhibitory synapses surrounding pyramidal neuron soma are made by densely arborized axons of basket interneurons expressing parvalbumin or cholecystokinin (Freund 2003; Foldy et al. 2007; Freund and Katona 2007) during postnatal development (Chattopadhyaya et al. 2004, 2007; Hartwich et al. 2009; Pangratz-Fuehrer and Hestrin 2011). To investigate a role for NCAM in perisomatic innervation, GABAergic interneurons of WT and homozygous NCAM null mutant mice were analyzed in layers II/III of the developing cingulate cortex, where most inhibitory input to pyramidal neurons occurs perisomatically (Xu et al. 2010). Development of perisomatic synaptic puncta was assessed during maturation on postnatal days 10 and 21 (P10 and P21), and at P60, when adult levels of synapses are attained (Brennaman and Maness 2008), by immunostaining for GAD65, a marker that is enriched in presynaptic GABAergic terminals (Feldblum et al. 1993; Esclapez et al. 1994). The mean number of GAD65-positive fluorescent puncta per soma and puncta area were quantified at each stage in the cingulate cortex (layers II/III) using established methods for analysis of synapse number in sections of mouse cerebral cortex (Chattopadhyaya et al. 2004, 2007; Di Cristo et al. 2004). The mean number and puncta area of perisomatic synapses increased postnatally from P10 to P60 in WT mice (Fig. 1; one-way ANOVA by genotype across all ages: $P < 0.005$), consistent with previous findings (Blue and Parnavelas 1983; Micheva and Beaulieu 1997; Chattopadhyaya et al. 2004). Notably, the mean number of perisomatic puncta also increased from P10 to P60 in NCAM null mutant mice but showed a small but significantly greater increase in NCAM null mutants compared with WT littermates at P21 and P60 (Fig. 1*A*,*B*). In addition, the size of perisomatic puncta was greater in NCAM null mutants than WT at each age (Fig. 1*C*). Immunofluorescent staining for parvalbumin indicated that the increase in number of perisomatic synapses per soma in layer II/III of the NCAM null cingulate cortex was not due to an increased density of parvalbumin-positive basket and chandelier cells, which target the soma and axon initial segment, respectively (NCAM null: 111 ± 14 cells/mm^2, WT: 107 ± 8 cells/mm^2; *t*-test, $P > 0.1$). These results suggest that postnatal maturation of perisomatic synapse number and size in GABAergic basket interneuron presynaptic

Downloaded from https://academic.oup.com/cercor/article/23/1/162/331609 by guest on 08 August 2022

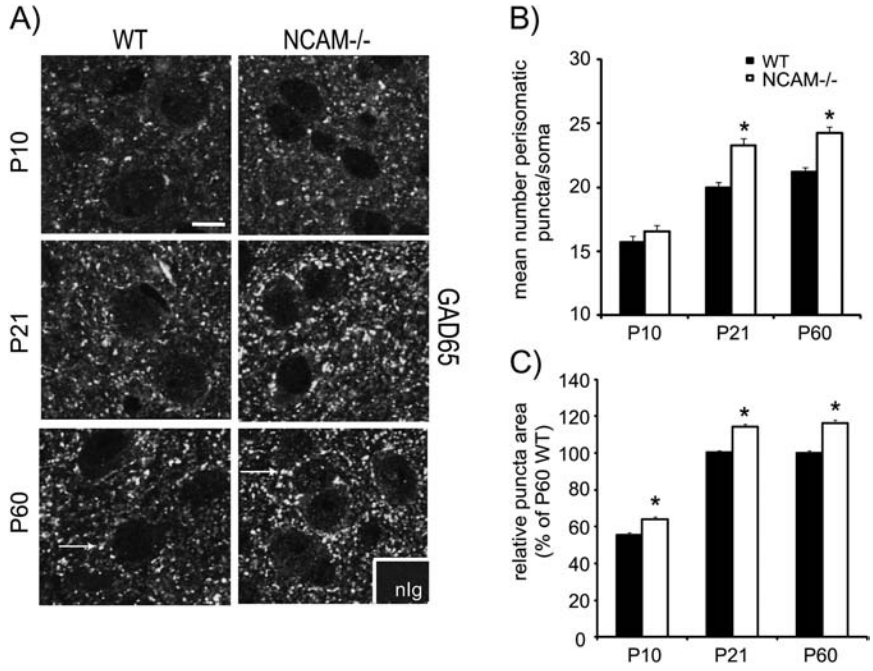

Figure 1. Loss of NCAM increases the number of perisomatic synapses of GABAergic interneurons in the cingulate cortex. (*A*) Immunofluorescence staining of GAD65 in GABAergic interneurons of the cingulate cortex (layer II/III) showed increased labeling of perisomatic synaptic puncta (arrows) during postnatal maturation of WT and NCAM null littermates (P10–P60, $n = 3$–5 mice/genotype per stage), with greater labeling in NCAM null mutants. Inset box shows a nonimmune IgG control staining. Single confocal images were taken using the same settings for each genotype. Scale bar: 10 μm. (*B*) The mean number of GAD65-labeled perisomatic puncta per soma section was significantly increased in the NCAM null mutant cingulate cortex compared with WT (P10–P60; *t*-test at each age, $^*P < 0.005$). (*C*) The mean area of GAD65-labeled perisomatic synaptic puncta, expressed as percent of WT, was significantly increased in NCAM null mutant cingulate cortex (P10–P60; *t*-test, $^*P < 0.005$).

terminals is under regulatory control by NCAM in the cingulate cortex.

The increased number and size of perisomatic puncta in the NCAM null mice could result in enhanced GABAergic inhibitory neurotransmission in cortical pyramidal cells. To test this, we recorded mIPSCs from pyramidal neurons in layer II/III of cingulate cortex of WT and NCAM null mice (P21–P27). mIPSCs are an indicator of the characteristics of GABAergic synapses and measure changes in inhibition at the synapse level through spontaneous GABA release. The amplitude, frequency, 10–90% rise time, and decay-time constant of individual events were measured and averaged within cells. Representative current traces for each genotype are shown in Figure 2*A*. The mIPSCs detected in this experiment are expected to arise from terminals distributed both perisomatically and in proximal dendritic regions. The measured average mIPSC time course for a given cell will then reflect the mean electrotonic distance of those terminals, weighted by their event frequency. Since there were more labeled perisomatic puncta in NCAM null mice, we hypothesized that the mIPSCs would be larger than in WT mice. The mean mIPSC amplitude in NCAM null mice (21.9 ± 1.1 pA) was significantly greater than in WT mice (18.4 ± 1.6 pA) (Fig. 2*B*; one-tailed *t*-test, $P = 0.048$; $n = 12$ NCAM null neurons, 10 WT neurons). In addition, the 10–90% rise time was significantly decreased in NCAM mutant mice (Fig. 2*B*; NCAM null: 0.440 ± 0.026 ms, WT: 0.557 ± 0.040 ms; two-tailed *t*-test, $P = 0.022$). Surprisingly, given the increase in terminal number, there was no significant change in mIPSC frequency (Fig. 2*B*). While there was a trend toward a decreased decay-time constant in NCAM null mice, the difference was not significant. Terminals on or near the soma should produce larger and faster rising mIPSCs, assuming that the conductance for all IPSCs has the same time course (Salin and Prince 1996; Banks et al. 1998), an effect that will be apparent even in voltage clamp due to limited spatial reach of the clamp in extended cells (Williams and Mitchell 2008). Indeed, the average mIPSC amplitudes were significantly correlated with rise time (Fig. 2*C*) in both WT and NCAM null mice (WT: $r = 0.66$, two-tailed *t*-test, $P = 0.040$; NCAM null: $r = 0.62$, two-tailed *t*-test, $P = 0.031$), such that larger mIPSCs had faster rise times, and the largest mIPSCs and fastest rise times were seen in the NCAM null mice. Similarly, decay- time constants were correlated with rise times for individual cells in the NCAM null mice (Fig. 2*D*; $r = 0.63$, two-tailed *t*-test, $P = 0.027$) but not in WT mice ($r = 0.25$, $P = 0.48$). The shorter rise time and larger amplitudes of mIPSCs, in combination with the increase in perisomatic synaptic puncta in NCAM null mutant mice, suggest that NCAM can modulate the strength of perisomatic synaptic inhibition onto pyramidal neurons.

Increased Perisomatic Synapses of GABAergic Interneurons in the Cingulate Cortex of EphrinA and EphA3 Null Mutant Mice

In addition to its well-known role in repellent axon guidance, ephrinA5/EphA signaling promotes proper columnar architecture and regulates growth of axon collaterals from pyramidal neurons within specific cortical layers (Castellani et al. 1998; Torii et al. 2009), suggesting that ephrinA/EphA signaling has the potential to regulate cortical interneuron arborization and synapse development. EphrinA2, -3, and -5 are the principal ephrinAs expressed in developing rodent forebrain, with ephrinA5 being the most prominent postnatally (Mackarehtschian et al. 1999; Yun et al. 2003; Depaepe et al. 2005; Torii et al. 2009). Perisomatic

Downloaded from https://academic.oup.com/cercor/article/23/1/162/331609 by guest on 08 August 2022

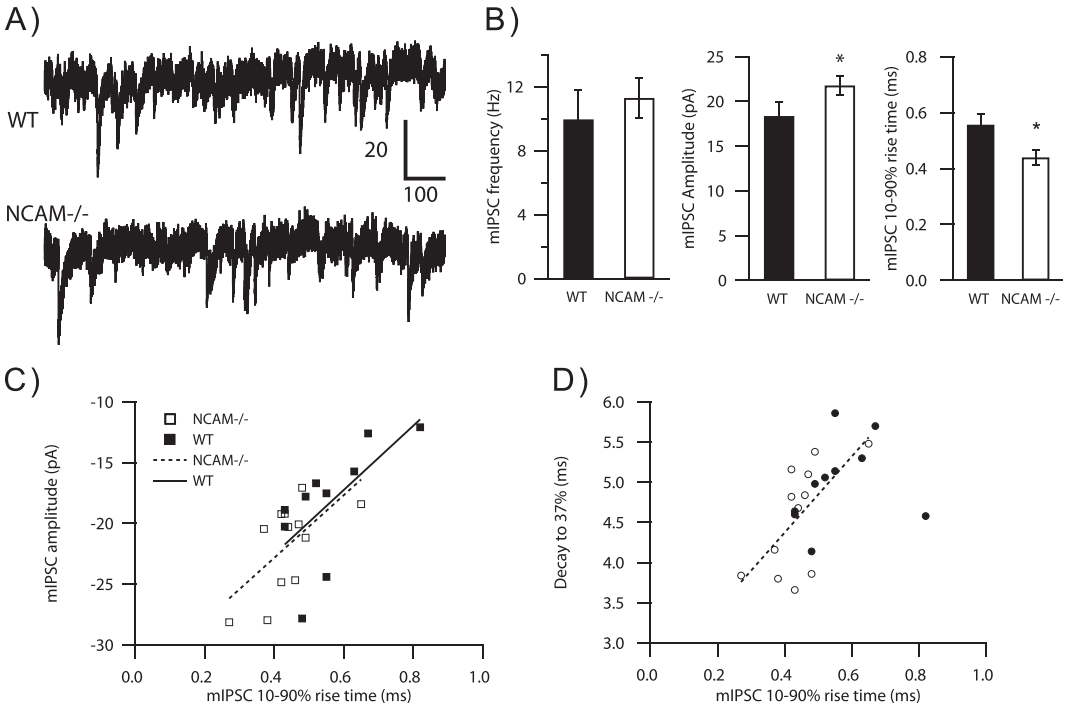

Figure 2. Increased amplitude and faster mIPSC time course in cingulate cortex of NCAM null mutant mice. (*A*) Representative current traces from pyramidal neurons in layers II/III of cingulate cortical slices from WT and NCAM null mutant mice. The calibration bar indicates pA and ms. Data low-pass filtered at 1 kHz. (*B*) Left: the frequency of mIPSCs was not significantly different in NCAM null and WT mice. Middle: the amplitude of mIPSCs in NCAM null mice was increased compared with WT (one-tailed *t*-test, $P < 0.05$). Right: the 10–90% rise time of mIPSCs in NCAM mice was faster compared with WT ($P < 0.05$). (*C*) The mIPSC amplitude was significantly correlated with the rise time in individual pyramidal cells for both NCAM null and WT mice (two-tailed *t*-test, $P < 0.05$), consistent with different average electrotonic distances of inhibitory synapses in individual cells. (*D*) The mIPSC decay-time constant was significantly correlated with the rise time in NCAM null but not WT pyramidal cells (two-tailed *t*-test, $P < 0.05$).

synaptic boutons of GABAergic axon arbors in the cingulate cortex (layer II/III) of WT and null mutant mice lacking ephrinA2/3/5, ephrinA5, or ephrinA3 were labeled by immunostaining for GAD65 at P21, the period of maximal perisomatic synaptogenesis in the mouse cingulate cortex (Brennaman and Maness 2008). The mean number of GAD65-positive perisomatic puncta per soma was significantly increased in ephrinA2/3/5 triple mutants and to a lesser extent ephrinA5 and ephrinA3 single mutants compared with WT (Fig. 3*A,B*). The size of perisomatic puncta in all mutant genotypes was also increased compared with WT and was greatest in the triple mutant (Fig. 3*C*). Labeling for a distinct GABAergic terminal marker, GAT-1, showed similar increases in puncta number and area in the cingulate cortex of ephrinA2/3/5, ephrinA5, and ephrinA3 mice compared with WT (not shown).

EphA3-7 receptors bind ephrinA2, -3, and -5, which are expressed in postnatal rodent cortex in distinct complex patterns (Mackarehtschian et al. 1999; Yun et al. 2003). Among the receptors, EphA3 preferentially binds to ephrinA5 (Smith et al. 2004). EphA3 null mice exhibited increased numbers and sizes of GAD65-positive perisomatic puncta from P21 through adulthood (P120) compared with WT mice (Fig. 3*B,C*). In contrast, the number of puncta in cingulate cortex of adult EphA4 mutant mice (P45) (Orioli et al. 1996) did not appear to be significantly different from WT (not shown).

Immunofluorescence staining for parvalbumin indicated that the elevated synaptic numbers in ephrinA and EphA3 mutant mice were not due to increased numbers of parvalbumin-positive neurons in the cingulate cortex (layers II/III; P21), as these were not different in ephrinA2/3/5 null (111 ± 4 cells/mm^2) or EphA3 null mutants (127 ± 14 cells/mm^2) compared with WT mice (110 ± 10 cells/mm^2; *t*-test, $P > 0.1$). Therefore, ephrinA2/3/5, EphA3, and NCAM null mutants displayed a common phenotype of increased number and size of GAD65-positive perisomatic presynaptic terminals in layer II/III of the cingulate cortex, consistent with a potentially cooperative role in postnatal development of basket interneurons.

NCAM Is Required for EphrinA5-Induced Growth Cone Collapse in GABAergic Interneurons

The increase in GABAergic perisomatic inhibitory synapses in NCAM-, ephrinA-, and EphA3-null mutant mice suggested that NCAM may interact with the ephrinA/EphA3 system to negatively regulate inhibitory connectivity during development. Growth cone collapse is a well-established paradigm for assessing ephrinA5 repellent signaling in developing axons and for testing potential modulators of ephrinA5 signaling (Wong et al. 2004; Dudanova et al. 2010; Demyanenko et al. 2011). We investigated growth cone collapse induced by ephrinA5-Fc fusion protein in GABA-expressing interneurons in dissociated cortical neuron cultures from WT and NCAM null mutant mice (P0) to investigate whether NCAM mediated ephrinA-induced repellent signaling during axon extension as a potential mechanism for restraining the number of inhibitory synapses. Neurons were allowed to extend neurites for 48 h in vitro, and were then treated with ephrinA5-Fc or control IgG for 30 min. Cultures were fixed and immunofluorescently stained for GABA to identify interneurons, which represent ~20% of neurons in these cultures (Waagepetersen et al. 2002) (Fig. 4*A*). Growth

Downloaded from https://academic.oup.com/cercor/article/23/1/162/331609 by guest on 08 August 2022

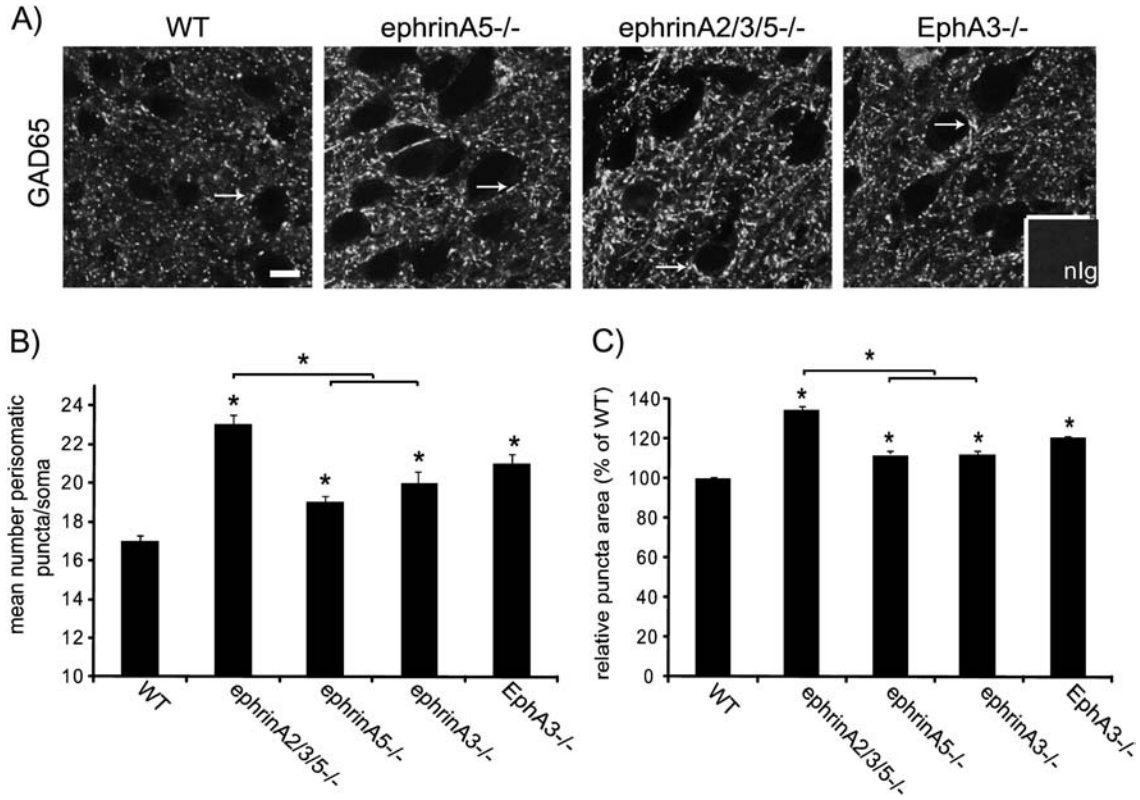

Figure 3. Loss of EphrinA or EphA3 increases the number and size of perisomatic synapses of GABAergic interneurons in the cingulate cortex. (*A*) Immunofluorescence staining for GAD65 in the cingulate cortex (layer II/III) of WT, ephrinA5-, ephrinA2/3/5-, and EphA3-null mice (P21, $n = 3$–5 mice per genotype) showed increased labeling of perisomatic synaptic puncta (arrows) in all mutant genotypes. Scale bar: 10 μm. (*B*) The mean number of GAD65-labeled perisomatic puncta per soma section was significantly increased in the cingulate cortex of ephrinA2/A3/A5-, ephrinA3-, ephrinA5-, and EphA3-null mice compared with WT and in triple mutants compared with either single mutant (*t*-test, $^*P < 0.005$). (*C*) The mean area of GAD65-labeled perisomatic synaptic puncta, expressed as percent of WT, was significantly increased in cingulate cortex of all mutant genotypes compared with WT and in triple mutants compared with either single mutant (*t*-test, $^*P < 0.005$).

cones were visualized by labeling F-actin with rhodamine-conjugated phalloidin and scored as collapsed (Fig. 4*A*, arrowhead) versus noncollapsed (Fig. 4*A*, arrow) by established morphological criteria (Cox et al. 1990). EphrinA5-Fc induced a strong growth cone collapse response in WT GABA-expressing neurons compared with control IgG treatment (Fig. 4*B*). There was no difference in the percent of collapsed growth cones in control IgG-treated cultures of WT and NCAM null interneurons. In contrast to its robust effect on WT interneurons, ephrinA5-Fc did not elicit significant growth cone collapse in GABA-expressing neurons from NCAM null mice (Fig. 4*B*). Growth cone collapse to ephrinA5 in GABA-negative cortical neurons was measured in the same cultures to determine if the effect was limited to interneurons. EphrinA5 also induced growth cone collapse in GABA-negative neurons of WT but not NCAM null cultures (Fig. 4*C*). These results demonstrated a requirement for NCAM in the mechanism of ephrinA5-induced growth cone collapse of GABAergic and non-GABAergic cortical neurons.

EphrinA Constrains Perisomatic Synapse Development by Basket Interneurons Through PSA-NCAM

To directly test whether ephrinAs could limit the development of perisomatic GABAergic synapses, organotypic slice cultures were prepared from the cingulate cortex of BAC transgenic mice (P5) that express EGFP from the GAD67 promoter (Chattopadhyaya et al. 2004) in a subpopulation of basket cells (Xu et al. 2010). Development of basket cells has been characterized in slices of visual cortex from these mice (Chattopadhyaya et al. 2004, 2007; Di Cristo et al. 2004, 2007), but the cingulate cortex, which has distinctive growth and gene expression profiles (Hoch et al. 2009), has not been studied. EGFP-labeled basket cells in WT cingulate cortex elaborated processes that increasingly arborized and formed perisomatic boutons over 14 DIV (Supplementary Fig. 1; one-way ANOVA $P < 0.05$) with a time course similar to that described in vivo (Brennaman and Maness 2008). At 14 DIV, WT cingulate slice cultures were treated with ephrinA5 fused to alkaline phosphatase (ephrinA5-AP) or AP control protein for 1 h. Addition of ephrinA5-AP to WT slice cultures elicited a small but significant decrease in the mean number of perisomatic boutons (Fig. 5*A*,*B*). To determine if a longer treatment with ephrinA5-AP would have a similar effect on perisomatic bouton number, separate slice cultures were treated with ephrinA5-AP or AP control for 6 days beginning at 8 DIV and continuing through 14 DIV. Perisomatic bouton numbers from these cultures decreased similarly compared with those treated with ephrinA5-AP for 1 h with no significant differences between the 2 time points (*t*-test, $P > 0.05$), suggesting that ephrinA5 can rapidly remodel inhibitory perisomatic boutons. To ask whether NCAM loss affected ephrinA5-induced remodeling of basket synapses, cingulate slice cultures from NCAM null mutant mice intercrossed with GAD67-EGFP reporter mice were similarly treated with ephrinA5-AP or control AP protein for 1 h at 14 DIV or 6 days

Downloaded from https://academic.oup.com/cercor/article/23/1/162/331609 by guest on 08 August 2022

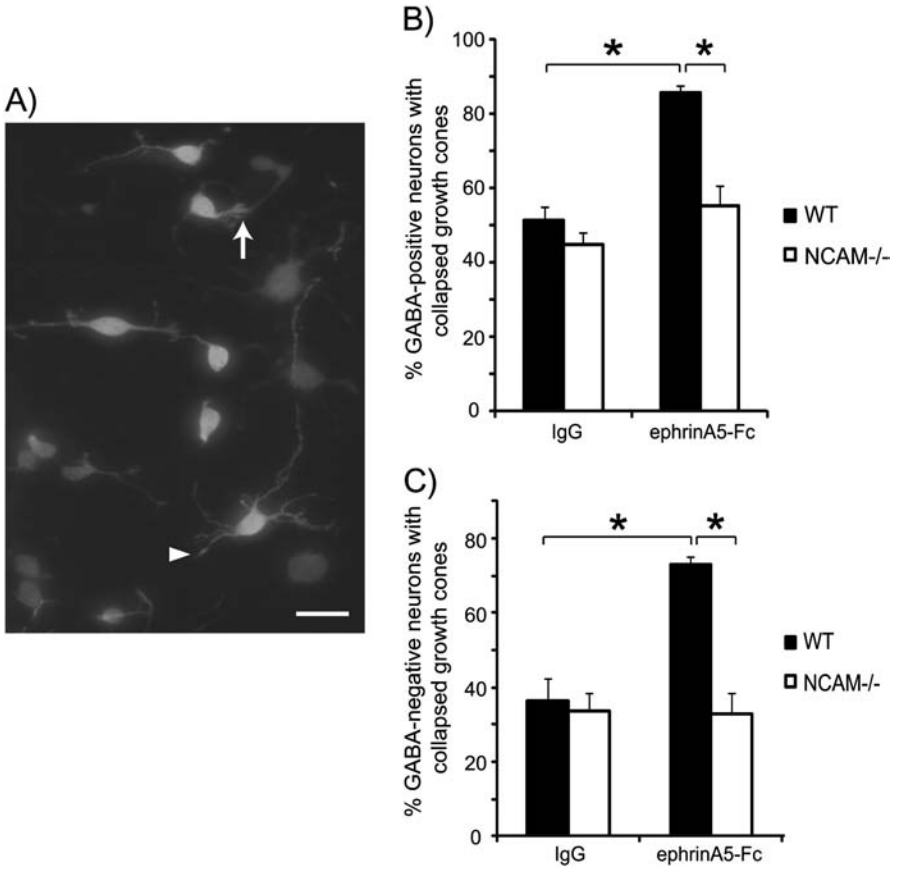

Figure 4. NCAM mediates EphrinA5-induced growth cone collapse of GABAergic and non-GABAergic interneurons. (*A*) Dissociated cortical neurons from WT or NCAM null mice (P0) were allowed to extend neurites for 48 h prior to the addition of ephrinA5-Fc or IgG control (3 μg/mL, 30 min) and stained for GABA- and rhodamine-conjugated phalloidin to visualize growth cone collapse in GABAergic cells. Representative image of ephrinA5-Fc–treated WT cultures illustrates GABA-labeled interneurons. Collapsed (arrowhead) and noncollapsed growth cones (arrow) are indicated. Scale bars: 10 μm. (*B*) Quantification of the percent of GABA-expressing neurons with collapsed growth cones in response to IgG or ephrinA5-Fc treatment in WT and NCAM null cultures ($n \geq 300$ growth cones per condition from 3 to 5 separate animals; *t*-test, $^*P < 0.05$). (*C*) Quantification of the percent of GABA-negative (excitatory) neurons with collapsed growth cones in response to IgG or ephrinA5-Fc treatment in WT and NCAM null cultures ($n \geq 300$ growth cones per condition from 3 to 5 separate animals; *t*-test, $^*P < 0.05$).

beginning at 8 DIV. EGFP-labeled basket interneurons in NCAM minus cingulate slices treated with control AP protein showed a small but significant increase in mean number of perisomatic boutons (Fig. 5*A,B*) compared with WT at both time points. However, ephrinA5-AP was unable to decrease the number of perisomatic boutons in NCAM minus basket cells (Fig. 5*A,B*).

EphrinA5-AP also decreased neurite length and branching (number of nodes) of WT basket interneurons in cultures treated for 6 days (Fig. 5*C–E*: neurite length, one-way ANOVA $P < 0.01$; number of nodes, *t*-test $P < 0.005$). NCAM null basket cells displayed significantly increased neurite length and number of nodes compared with WT basket interneurons (Fig. 5*C–E*: neurite length, one-way ANOVA $P < 0.005$; number of nodes, *t*-test $P < 0.005$). Although there was a trend toward decreased arborization of NCAM null basket cells with ephrinA5-AP, this was not significant (neurite length, one-way ANOVA $P > 0.05$; number of nodes, *t*-test $P > 0.1$). Acute treatment with ephrinA5 (1 h) produced no effect on neurite arborization in WT or NCAM null basket cells (not shown). These results indicate a cooperative role for ephrinA5 and NCAM in limiting perisomatic boutons and restricting arborization of basket cell interneurons.

NCAM is predominantly expressed in a polysialylated form in mice from embryonic stages through P10, with lower levels present until P21 (Brennaman and Maness 2008). Therefore, NCAM is polysialylated to some degree during the time course of the slice culture assays. The lack of effect of ephrinA5 in NCAM null cultures could be due to a lack of PSA since NCAM is the principal carrier of PSA in mammalian brain (Colley 2010; Galuska et al. 2010; Hildebrandt et al. 2010; Rey-Gallardo et al. 2010). In visual cortex, removal of PSA leads to precocious maturation of interneurons and early onset of the critical period (Di Cristo et al. 2007). In WT GAD67-EGFP cingulate cortex (layers II/III), PSA immunoreactivity was observed in a diffuse punctate pattern localizing in part with EGFP-labeled basket cells (Fig. 5*F*). To assess the contribution of PSA to ephrinA5-induced remodeling of basket cells in cingulate cultures, cultures from GAD67-EGFP mice were treated with endoneuraminidase-N (endo-N) at 6 DIV to remove PSA from NCAM prior to ephrinA5-AP or AP control addition for 1 h or 6 days. Endo-N efficiently removed PSA in these cultures (Fig. 5*F*). Endo-N–treated cultures displayed no difference in the number of perisomatic boutons compared with untreated cultures (Fig. 5*G*). Addition of ephrinA5-AP to endo-N–treated cultures had no effect on puncta number (Fig. 5*G*). Similarly, endo-N treatment produced neurite length distributions and branching values similar to the untreated controls (mean

Downloaded from https://academic.oup.com/cercor/article/23/1/162/331609 by guest on 08 August 2022

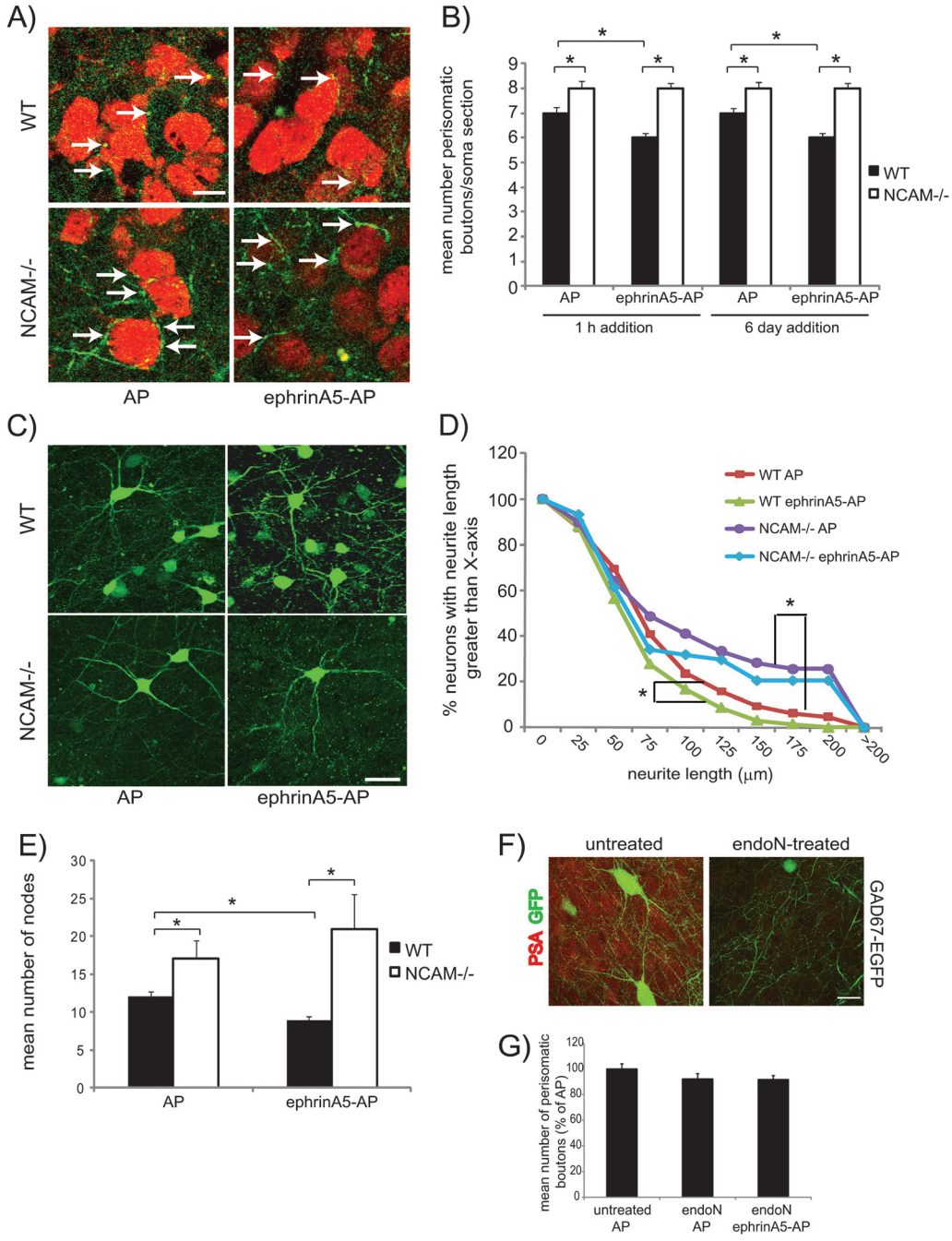

Figure 5. PSA-NCAM mediates EphrinA5-induced remodeling of perisomatic innervation and arborization of basket interneurons in culture. (*A*) Slice cultures (400 μm) of cingulate cortex from GAD67-EGFP mice (P5) were cultured for 14 DIV at which time ephrinA5-AP or AP proteins (5 μg/mL) were added for 1 h. Alternatively, slices were cultured for 8 DIV at which time ephrinA5-AP or AP control (5 μg/mL) were added every other day until 14 DIV (6 day addition). Cultures were immunofluorescently labeled for NeuN (red) and EGFP (green) to visualize synaptic puncta. Representative images from single confocal planes of WT and NCAM null slices treated with AP or ephrinA5-AP for 1 h are shown. Arrows indicate perisomatic synaptic puncta onto NeuN-labeled neurons. Scale bar: 10 μm. (*B*) Mean number of perisomatic synapses per soma section was plotted per condition (n = 60–600 neurons per condition; t-test, $^*P < 0.05$). Three to 5 slices per mouse per genotype were used in each case (n = 3–5 mice). (*C*) Basket cells from layer II/III of WT and NCAM null cingulate cortex were fully imaged through z-stacks and reconstructed with Neurolucida software. Representative images of reconstructed GAD67-EGFP basket interneurons from WT and NCAM null mice treated with AP or ephrinA5-AP for 6 days are shown (n = 3–5 slices per mouse per genotype, 3–5 mice per genotype, 60–180 neurons per condition analyzed). Scale bar: 10 μm. (*D*) Cumulative total neurite length per neuron was plotted as a percentage of neurons with length greater than the length indicated on the x-axis. Significant differences were observed between WT slices treated with AP versus ephrinA5-AP and between each type of WT slice and NCAM null slices (ANOVA, $P < 0.01$). No differences were observed between NCAM null slices treated with AP or ephrinA5-AP. (*E*) Mean number of nodes (branch points) was plotted for per condition (t-test, $^*P < 0.05$). (*F*) Representative images of single confocal planes from endo-N–treated and endo-N–untreated slices. PSA is present in a diffuse pattern that partly colocalized with EGFP in untreated cultures (left). Endo-N efficiently removed PSA signal from slice cultures (right). Scale bar = 10 μm. (*G*) Mean number of perisomatic synapses per soma section was plotted per condition (n = 60–600 neurons per condition) for slices treated for 1 h with ephrinA5-AP or AP control. Three to 5 slices per mouse per condition were used in each case (n = 3–5 mice). No significant differences were observed (t-test, $P > 0.05$).

Downloaded from https://academic.oup.com/cercor/article/23/1/162/331609 by guest on 08 August 2022

number of nodes control: 18 ± 2; endo-N: 16 ± 2), with no effect upon ephrinA5-AP treatment (mean number of nodes: 21 ± 2; not shown). The lack of response of basket cells to ephrinA5-AP in endo-N–treated slices was similar to the NCAM null cultures and suggested that PSA-NCAM enables ephrinA5-induced restriction of basket cell arborization, neurite growth, and perisomatic puncta.

NCAM and EphA3 Colocalize at Perisomatic Synaptic Puncta and Form a Complex in Postnatal Forebrain

The similarity in phenotype of GABAergic perisomatic synapses between NCAM, EphA3, and ephrinA null mutant mice and the functional role for NCAM in ephrinA5-induced repellent responses of basket interneurons raised the possibility that NCAM and EphA3 may form a functional complex in vivo. First, immunofluorescent staining for EphA3 was performed in cingulate cortex (layer II/III) of P21 GAD67-EGFP mice to determine whether EphA3 was expressed in the basket cells analyzed in slice cultures. EphA3 localized to soma, neuropil (n), and perisomatic puncta (p) of EGFP-positive basket interneurons (Fig. 6*A*). NCAM has been shown previously to be expressed in GAD67-EGFP–positive basket cell boutons and to colocalize with GAD65 (Pillai-Nair et al. 2005). To determine if NCAM colocalized with EphA3 in postnatal mouse brain, double immunofluorescence staining for NCAM140/180 and EphA3 was performed in cingulate cortex (layer II/III) of WT mice at P21. EphA3 immunoreactivity was prominent in the neuropil and somata of cells with pyramidal neuron morphology (Fig. 6*B*). NCAM was also present in the neuropil but was undetectable throughout most of the soma. NCAM and EphA3 appeared to colocalize at or near the soma membrane, as seen in merged images. NCAM and EphA3 colocalized at the perisomatic margin (p) in a punctate pattern and at puncta within the neuropil (higher magnification, outset boxes) as seen in merged images. In controls, EphA3 antibodies did not label the cingulate cortex of EphA3 null mice (Fig. 6*B*, inset box), and nonimmune IgG did not stain WT sections (Fig. 6*A*,*D*, inset boxes). In contrast to the robust levels of NCAM observed, PSA was expressed at much lower levels in P21 cingulate cortex in a diffuse punctate pattern in close apposition to EphA3 (Fig. 6*C*).

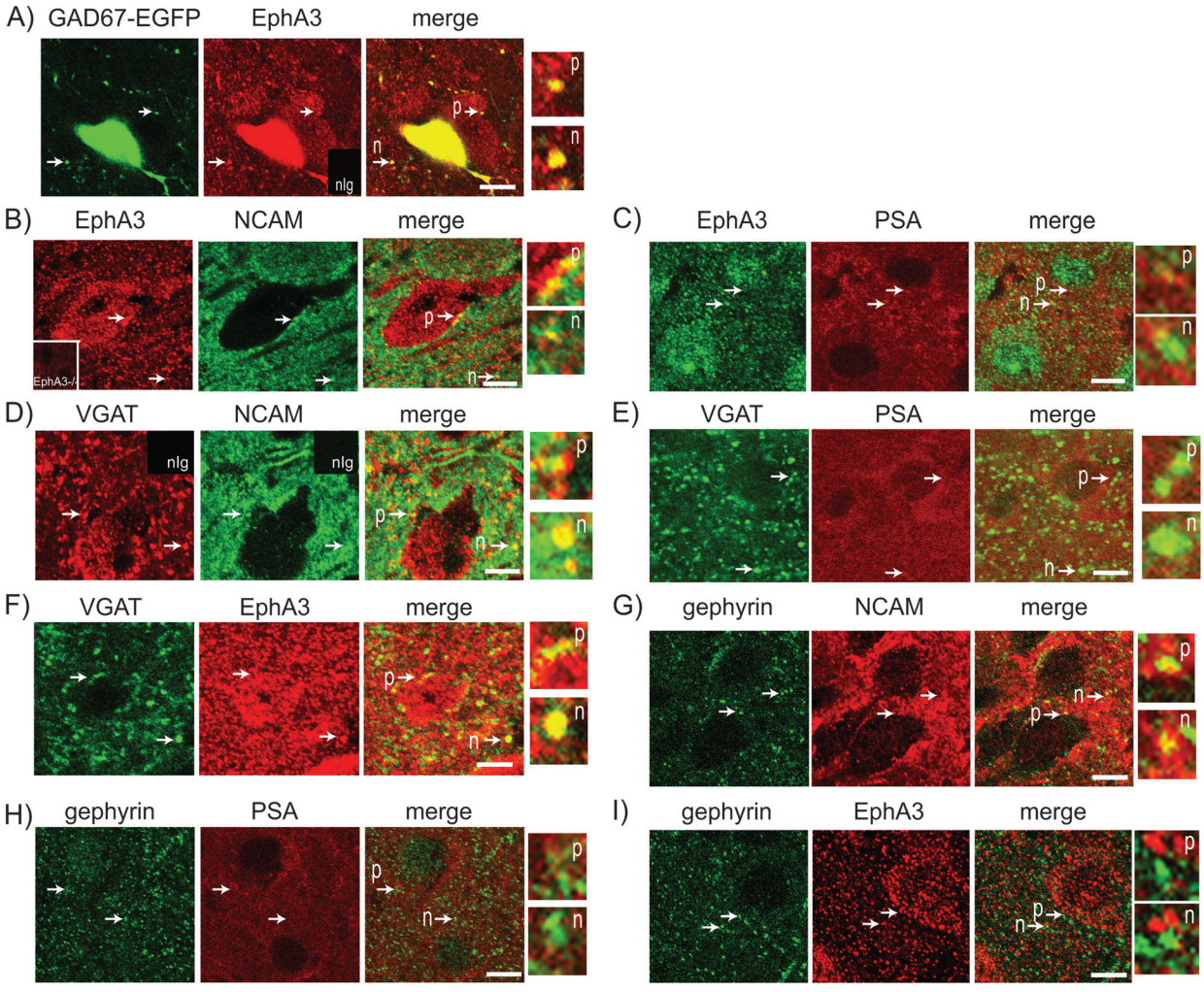

Figure 6. NCAM and EphA3 colocalize at presynaptic perisomatic puncta. Cingulate cortex of WT mice (P20–P23) was immunofluorescently stained and imaged by confocal microscopy. Arrows indicate perisomatic puncta (p) or neuropil (n) and are shown in higher magnification in outset boxes. A representative nonimmune IgG control (nIg) is shown in panel (*A,D*). Scale bar = 10 μm. Double immunofluorescence labeling for GFP and EphA3 in WT GAD67-EGFP mice (*A*). Staining of EphA3 null mutant cortex with EphA3 antibody or WT cortex with normal Ig (nIg; inset boxes) showed no significant labeling. Double immunofluorescence labeling for EphA3 and NCAM (*B*), EphA3 and PSA (*C*), VGAT and NCAM (*D*), VGAT and PSA (*E*), VGAT and EphA3 (*F*), gephyrin and NCAM (*G*), gephyrin and PSA (*H*), and gephyrin and EphA3 (*I*).

Downloaded from https://academic.oup.com/cercor/article/23/1/162/331609 by guest on 08 August 2022

To better define the presynaptic versus postsynaptic localization for NCAM, PSA, and EphA3 at inhibitory synapses, double immunofluorescence staining was performed using antibodies to NCAM, PSA, or EphA3 and either VGAT (inhibitory presynaptic) or gephyrin (inhibitory postsynaptic) in WT cingulate cortex (layer II/III) at P21. Both NCAM (Fig. 6*D*) and EphA3 (Fig. 6*F*) colocalized with VGAT at presynaptic perisomatic puncta (p) and in puncta within the neuropil (n). In contrast, NCAM (Fig. 6*G*) colocalized with the postsynaptic marker gephyrin at perisomatic puncta and neuropil at lower levels, while no discernable EphA3 colocalization was observed (Fig. 6*I*). PSA was observed surrounding VGAT- (Fig. 6*E*) and gephyrin-positive (Fig. 6*H*) perisomatic puncta and neuropil, similar to the localization of NCAM. Taken together, these results are consistent with colocalization of EphA3, PSA, and NCAM140/180 at presynaptic perisomatic synaptic terminals and neuropil of GABAergic interneurons. A small amount of NCAM and PSA may additionally be present at inhibitory postsynaptic sites.

To identify the pattern of ephrinA5 expression in the cingulate cortex during perisomatic puncta development, ISH of ephrinA5 transcripts was performed at P15. EphrinA5 messenger RNA (mRNA) labeling was observed in the cingulate cortex (PFC), primary somatosensory (S1), and visual (V1) cortical areas (Fig. 7*A*). EphrinA5 transcripts were evident in all cortical layers (Fig. 7*B,D,E*). No labeling was observed with the control sense probe (Fig. 7*C*). At higher magnification, ephrinA5 mRNA labeling could be seen in soma of large cells with pyramidal neuron morphology (Fig. 7*F*, dashed lines) with no labeling by the control sense probe (Fig. 7*I*). Higher levels of ephrinA5 mRNA were observed in S1 and V1 as compared with the cingulate cortex (Fig. 7*B–H*). It was not possible to determine if smaller labeled soma represented other cell types, such as interneurons, astroglia, or pyramidal somal segments. The overall distribution of ephrin mRNA (Fig. 7*B,D,E*) was consistent with pyramidal neuron expression, in accord with previous reports in the cortical plate (E16-P7) (Castellani et al. 1998; Gao et al. 1998; Mackarehtschian et al. 1999) and atlas expression patterns (Max Planck Institute for Biophysical Chemistry, www.genepaint.org; and Allen Institute for Brain Science, http://developingmouse.brain-map.org). Although ephrinA5 may be expressed in several cell types in the cingulate cortex (Filosa et al. 2009), these results suggested that ephrinA5 in pyramidal neurons may interact with an EphA3/NCAM complex on basket cell processes to constrain perisomatic innervation.

Physical interaction between EphA receptors and transmembrane NCAM isoforms (140 and 180 kDa) was investigated

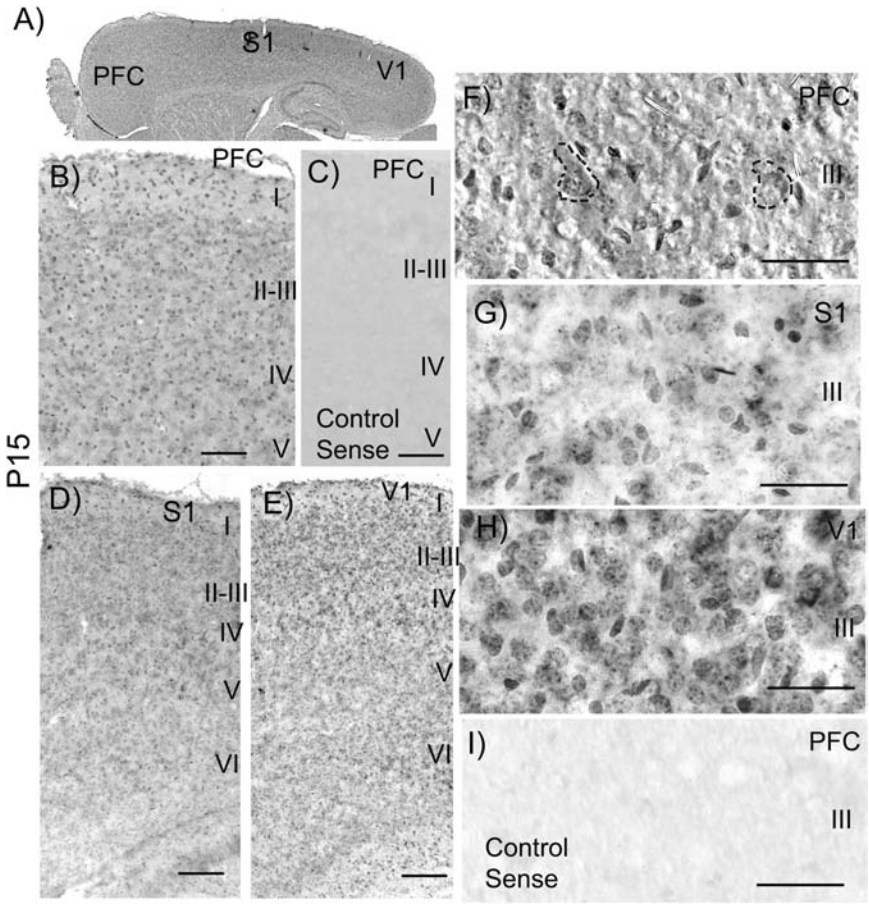

Figure 7. EphrinA5 localizes to pyramidal neurons. (*A*) EphrinA5 mRNA was detected ISH in the PFC and at somewhat elevated levels in primary somatosensory (S1) and visual (V1) areas at P15 using a digoxigenin antisense probe in sagittal sections. PFC labeling was enriched in layers II/III (*B*) as shown in comparison with the control sense probe (*C*). Increased levels of ephrinA5 mRNA were observed in S1 (*D*, high magnification—*G*) and V1 (*E*, high magnification—*H*) as compared with PFC. (*F*) Higher magnification in differential contrast images showed ephrinA5 mRNA labeling in soma of cells with pyramidal neuron morphology in layer III (green dashed lines), as well as in smaller soma, compared with sense probe labeling (*I*). Control sense probe labeling showed no detectable signal in S1 or V1 as well (not shown). Abbreviations: PFC—prefrontal cortex (cingulate cortex), S1—primary somatosensory cortex, and V1—primary visual cortex. Scale bars: 50 μm.

Downloaded from https://academic.oup.com/cercor/article/23/1/162/331609 by guest on 08 August 2022

by coimmunoprecipitation from mouse forebrain during the maximal period of interneuron synaptogenesis (P15–P21) to determine if the effects of NCAM and ephrinA5 on inhibitory synapses may be mediated by association of these proteins. Among NCAM isoforms, NCAM140 is preferentially localized to growth cones and axons of developing neurons, whereas NCAM180 is enriched at the postsynaptic membrane in mature neurons (Sytnyk et al. 2006). NCAM120, the GPI-linked isoform, is predominantly localized to glia. The postnatally expressed EphA receptors, EphA3, EphA4, and EphA7 (Mackarehtschian et al. 1999; Yun et al. 2003; Miller et al. 2006), were immunoprecipitated from postnatal forebrain lysates (P21) with specific antibodies, and coimmunoprecipitation of NCAM isoforms was examined by western blotting. NCAM140, and to a lesser extent NCAM180 and NCAM120, coimmunoprecipitated with EphA3 (135 kDa) at both stages (Fig. 8*A*). Only

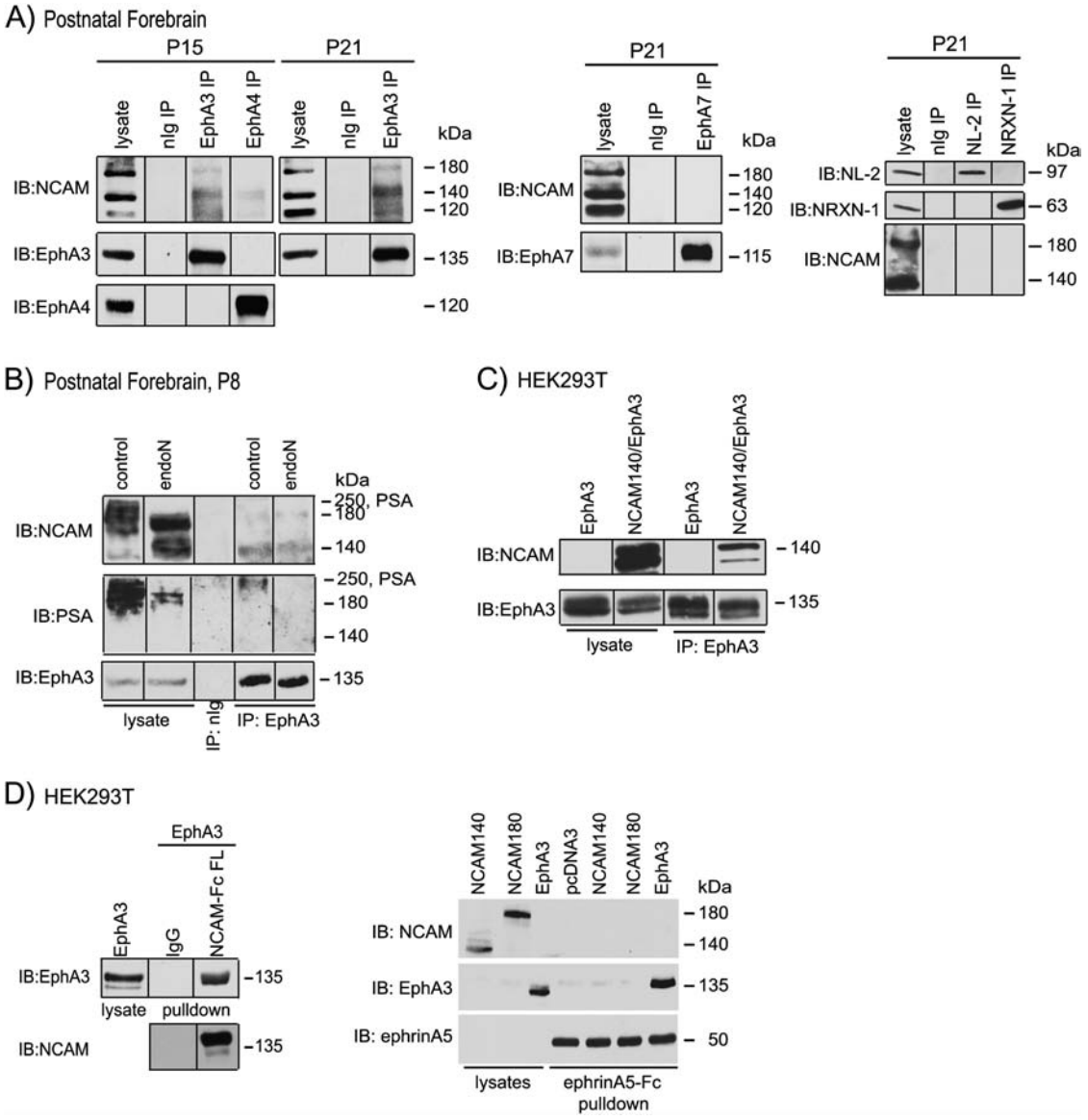

Figure 8. NCAM and EphA3 form a molecular complex that binds EphrinA5. (*A*) Forebrain lysates (1 mg) from WT mice (P15 and P21) were immunoprecipitated with nonimmune IgG (nIg) or antibodies to EphA3, EphA4, EphA7, Neuroligin 2 (NL-2), or Neurexin 1 (NRXN-1), as indicated. Proteins from immunoprecipitations or lysates were separated by SDS-PAGE and immunoblotted (IB) with the indicated antibodies. Note that in the first set of panels, the lysate for the NCAM immunoblot is from a shorter exposure time (1 min) than the other lanes (15 min), as individual bands from the lysates of the 15 min exposure were obscured by oversaturation of the signal. All other panels show lysates and immunoprecipitations from the same exposure times. (*B*) Freshly prepared forebrain lysates from P8 mice were treated with endo-N (40 U) for 1 h prior to immunoprecipitation with antibodies to EphA3 or nonimmune IgG (nIg). Untreated lysates from littermate mice were used as controls. Proteins from lysates or immunoprecipitations were immunoblotted for NCAM extracellular domain, PSA, or EphA3 antibodies. Note that the NCAM and PSA immunoblots are from shorter exposure times (5 s) than the IP lanes (1 or 10 min, respectively), as individual bands in the lysate were obscured by the longer exposures due to oversaturation of the signal. (*C*) HEK293T cells were cotransfected with NCAM140 and EphA3 cDNAs or with EphA3 alone. Lysates (500 μg) were immunoprecipitated with antibodies to EphA3, and IPs and lysates subjected to immunoblotting with antibodies to the NCAM intracellular domain (mAb OB11) or EphA3. In the NCAM immunoblot, the lysate is from a 10-s exposure and the immunoprecipitations from a 5-min exposure, as the longer exposure of the lysate obscured the individual bands. All lanes in the EphA3 immunoblot are from the same exposure time. (*D*) HEK293T cells were transfected with NCAM140, NCAM180, or EphA3 cDNAs alone. Cell lysates (500 μg) were incubated with ephrinA5-Fc (right) or NCAM-Fc (left) fusion proteins (2 μg) consisting of the entire extracellular domain and protein A/G agarose beads to detect protein/protein interactions via a pull-down assay. Proteins were immunoblotted with antibodies to the NCAM extracellular domain (pAb H300), EphA3 or ephrinA5. In all panels, all lanes are from the same gel and boxes outline lanes, which were cropped to remove duplicates.

Downloaded from https://academic.oup.com/cercor/article/23/1/162/331609 by guest on 08 August 2022

a small amount of PSA-NCAM (~200 to 250 kDa) was present at these stages, as indicated by a broader band above 180 kDa in lysates. PSA-NCAM did not appear to coimmunoprecipitate significantly with EphA3, as there was no discernible band above the NCAM180 band in the immunoprecipitations. Only a small amount of NCAM coimmunoprecipitated with EphA4 and none with EphA7 (Fig. 8*A*). NCAM also did not associate with Neurexin 1 (NRXN-1, presynaptic) and Neuroligin 2 (NL-2, postsynaptic), which are unrelated adhesion molecules present at developing inhibitory synapses (Fig. 8*A*).

To further investigate whether PSA-NCAM associated with EphA3, brain lysates from P8 mice, which express higher levels of PSA-NCAM than at later stages, were treated with endo-N for 1 h to remove PSA. At P8, NCAM was predominantly polysialylated with smaller amounts of non-PSA NCAM140 and NCAM180 present in the lysate (Fig. 8*B*). Endo-N treatment converted the broad ~200 to 250 kDa PSA-NCAM band to 140 and 180 kDa bands, representing the 2 major transmembrane isoforms of NCAM. Immunoblotting for PSA indicated that the majority of NCAM140 and NCAM180 in the endo-N–treated samples lacked PSA. However, there was a small amount of residual PSA (>180 kDa) in the lysate due to incomplete digestion (Fig. 8*B*). NCAM140, and to a much lesser extent, NCAM180, coimmunoprecipitated with EphA3 from non-treated control lysates. The NCAM species that associated with EphA3 were not recognized by PSA antibodies and continued to associate with EphA3 when immunoprecipitated from endo-N–treated lysates (Fig. 8*B*). An unidentified high molecular weight PSA species did coimmunoprecipitate with EphA3 from control but not endo-N–treated lysates (Fig. 8*B*). This species was not recognized by NCAM-specific antibodies in the immunoprecipitation lanes, in contrast to PSA-NCAM, which was readily detected in the lysates, suggesting that this high molecular weight species is distinct from NCAM. Also, it does not correspond in size to other polysialylated proteins present at lower levels in brain compared with PSA-NCAM, such as SynCAM1 (Galuska et al. 2010), and polysialyltransferases (Muhlenhoff et al. 1996; Close and Colley 1998). We also performed coimmunoprecipitation of NCAM140 and EphA3 from lysates of transfected HEK293T cells, where NCAM is not polysialylated. NCAM140 and smaller amounts of an NCAM cleavage fragment readily coimmunoprecipitated with EphA3 from transfected cell lysates (Fig. 8*C*). EphA3 immunoprecipitation from untransfected cells showed no NCAM. The 2 EphA3 bands may represent differentially glycosylated forms in HEK293T cells.

To determine whether the association of NCAM with EphA3 was mediated by binding determinants in the NCAM extracellular domain, HEK293T cells expressing EphA3 alone were preincubated with Fc fusion proteins comprising the full-length NCAM extracellular domain (NCAM-Fc) and complexes precipitated with Protein A/G agarose beads in pull-down assays. NCAM-Fc proteins efficiently bound EphA3 (Fig. 8*D*) and demonstrated an association between the NCAM extracellular domain and EphA3. An association of NCAM140 or NCAM180 with ephrinA5 was then investigated in pull-down assays in which ephrinA5-Fc was added to HEK293T cell lysates expressing NCAM140, NCAM180, or EphA3 as a control. Pull-down assays with Protein A/G agarose beads showed no association of NCAM140 or NCAM180 with ephrinA5-Fc, whereas ephrinA5-Fc readily bound to EphA3 (Fig. 8*D*). Trace amounts of endogenous EphA3 in HEK293T cells were pulled down with ephrinA5-Fc from cells transfected with pcDNA3, NCAM140, or NCAM180. Together, these results show that non-PSA NCAM140 associated preferentially with EphA3 through the extracellular domain of NCAM, without direct association with the ephrinA5 ligand.

Discussion

Here, we identified a novel mechanism governed by ephrinA/EphA3 and NCAM to regulate postnatal development of GABAergic basket interneurons in the mouse PFC. Genetic disruption of NCAM, EphA3, or ephrinA2/3/5 ligands in null mutant mice resulted in increased numbers of perisomatic inhibitory synapses, a large portion of which are derived from basket interneurons (Freund 2003; Foldy et al. 2007; Freund and Katona 2007), in layers II/III of the cingulate cortex. EphrinA5 treatment decreased basket cell arborization and synapse formation in GAD67-EGFP cortical slices and induced growth cone collapse in dissociated neurons, while loss of NCAM or PSA impaired ephrinA5-induced basket cell axon responses. A functional consequence of NCAM deletion was to increase in mIPSC amplitude and decrease mIPSC rise time, suggesting stronger inhibition arising from more proximally located synapses. This previously unrecognized role of ephrinA/EphA in GABAergic interneurons, and its modulation by PSA-NCAM, may serve to constrain inhibitory synapse formation, important for regulating excitatory/inhibitory balance in prefrontal circuits.

These results provide the first evidence to identify an ephrinA/EphA-dependent mechanism in inhibitory synapse development and implicate PSA-NCAM in enabling ephrinA5/EphA3-induced remodeling of basket cell synapses. Our findings suggest that PSA on NCAM is primarily responsible for enabling ephrinA5/EphA3-mediated remodeling, as NCAM null and endo-N–treated interneurons failed to respond to ephrinA5 stimulation. Whereas non-PSA NCAM readily associated with EphA3, PSA-NCAM did not, implying that PSA has an indirect effect on ephrinA5/EphA3-induced remodeling. PSA-NCAM diminishes progressively between P10 and P20 in mouse forebrain (Brennaman and Maness 2008), concomitant with the appearance of perisomatic synapses. However, NCAM null but not endo-N–treated interneurons displayed increases in neurite growth, branching, and perisomatic puncta in slices, suggesting interaction of non-PSA NCAM with EphA3 or other partners (Niethammer et al. 2002; Panicker et al. 2003; Paratcha et al. 2003) may contribute to constraint of interneuron arbors. Similarly, loss of PSA in mice lacking polysialyltransferases causes some defects not shared with mice lacking NCAM (Weinhold et al. 2005). In accord with our findings, PSA-NCAM prevents premature formation of perisomatic basket cell synapses in the visual cortex (Di Cristo et al. 2007) and limits connectivity of hippocampal axons during sensitive periods (Seki and Rutishauser 1998; Galimberti et al. 2010; Puchkov et al. 2011; Gomez-Climent et al. 2011). However, these studies did not identify the repellent ligand–receptor system responsible for constraining connectivity. By reducing NCAM-dependent interactions in basket cell terminals, PSA-NCAM may allow axons to respond to ephrinA5 through EphA3 signaling, thus promoting axon pruning and/or synapse remodeling.

The increase in inhibitory synapse numbers in the NCAM null cingulate cortex is likely responsible for the increased mIPSC amplitude and decreased rise time measured in cortical

Downloaded from https://academic.oup.com/cercor/article/23/1/162/331609 by guest on 08 August 2022

slices. These findings are consistent with an overall shift in the location of inhibitory synapses toward the soma. There are 2 consequences of altered inhibition in NCAM null mutants. First, the inhibition is potentially stronger in the mutants (depending on whether the mIPSC amplitude is accompanied by changes in release probability), which could reduce firing rates in the cortical network. Second, faster inhibition could affect the timing of network-based activity, including oscillatory events, such as gamma oscillations (White et al. 2000; Bartos et al. 2002), and thus disrupt the cooperative timing and firing of neurons that is thought to be necessary for normal cognitive functions (reviewed in Lewis et al. (2011)). Consistent with this idea, NCAM minus mice exhibit several behaviors that might be attributed to an imbalance in excitatory/inhibitory connectivity including increased intermale aggression (Stork et al. 1997), impaired contextual and cued fear conditioning (Senkov et al. 2006; Kochlamazashvili et al. 2010), increased anxiety in light/dark avoidance (Stork et al. 1999), and decreased anxiety on an elevated plus maze (Stork et al. 1999, 2000; Jurgenson et al. 2010). PSA has important consequences on behavior as well. Mice lacking the polysialyltransferase ST8SiaIV/PST display decreased social interaction (Calandreau et al. 2010), increased exploration, and impaired fear conditioning (Angata et al. 2004). Mice lacking another polysialyltransferase, ST8SiaII/STX, display decreased social motivation and increased aggression (Calandreau et al. 2010). Few behavioral or physiological studies have been performed on ephrinA or EphA3 null mice, but ephrinA2 null mice display impaired reversal learning in a visual discrimination maze task (Arnall et al. 2010). These results, paired with our findings, suggest that ephrinA/EphA and NCAM may have broad roles in regulating synapse development and function in the central nervous system.

Repellent signaling by ephrinA/EphA3 may also regulate the structural development of perisomatic inhibitory synapses. The increased size of GAD65-positive perisomatic puncta in NCAM, ephrinA2/3/5, and EphA3 null cingulate cortex is likely to represent an intermediate stage in maturation of basket cell synapses. GABAergic inhibitory synapses reach a peak size during the second to fourth postnatal week, after which time they contract to their mature size (Blue and Parnavelas 1983; Micheva and Beaulieu 1997; Chattopadhyaya et al. 2004; Pangratz-Fuehrer and Hestrin 2011). Two other repellent axon guidance molecules, Semaphorin3F and Neuropilin-2, similarly participate in restricting both the size and number of postsynaptic specializations at excitatory synapses (Tran et al. 2009). NCAM140/180, through its ability to engage the spectrin/actin cytoskeleton (Leshchyns'ka et al. 2003), may maintain the integrity of the postsynaptic density, as NCAM null (Puchkov et al. 2011) or endo-N–treated mice (Dityatev et al. 2004) exhibit increased numbers of perforated postsynaptic densities at excitatory synapses in the hippocampus. Larger synaptic puncta have also been observed in mice with mutations in genes encoding the cell adhesion molecules LRRTM1 (Linhoff et al. 2009), Neuroligin 3 (Tabuchi et al. 2007), and β-catenin, where they have been associated with dispersion of synaptic vesicles (Bamji et al. 2003).

Our findings suggest a model in which PSA-NCAM at pre- and/or postsynaptic sites reduces NCAM-dependent adhesion to promote branch retraction and synapse remodeling of basket cell axons through EphA3 in response to ephrinA5 on pyramidal cell soma. Removal of PSA during postnatal cortical development may increase NCAM-dependent adhesion, potentially inhibiting ephrinA/EphA-induced terminal retraction, either by stabilizing synaptic contact or by inhibitory interaction with EphA3. Such a model is consistent with findings that polysialylation of NCAM reduces affinity of intermolecular interactions (Johnson et al. 2005) and that ephrinA/EphA signaling is sensitive to adhesive force (Salaita and Groves 2010; Salaita et al. 2010). The proposed mechanism may critically regulate the number of perisomatic synapses to achieve an appropriate inhibitory–excitatory balance of connectivity in the PFC. Thus, mutations in genes encoding ephrinA/EphA signaling complexes (ephrinA5, EphA3), NCAM, or polysialyltransferases ST8SiaIV/PSA and ST8SiaII/STX have the potential to alter prefrontal cognitive functions relevant to neuropsychiatric disorders.

Supplementary Material

Supplementary material can be found at: http://www.cercor.oxfordjournals.org/

Funding

National Institutes of Health funding of the University of North Carolina Silvio O. Conte Center for the Neuroscience of Mental Disorders (MH064065 to P.F.M.); National Institute on Deafness and Other Communication Disorders (R01DC009809 to P.B.M.); and 2009 National Alliance for Research on Schizophrenia and Depression William Risser Charitable Trust Investigator/Young Investigator Award (L.H.B.).

Notes

We thank Kyle Brennaman for data analysis automation, Heather Decot, and Blaine Nesbitt for assistance with NCAM-Fc assays, Greg Lemke (The Salk Institute) for EphA4 null mice, David Feldheim (University of California, Santa Cruz) for helpful advice and ephrinA5 probe, Urs Rutishauser (Memorial Sloan-Kettering Cancer Center) for PSA 5A5 monoclonal antibody and endo-N, and Elena Pasquale (Burnham Institute, University of California San Diego) for plasmids. *Conflict of Interest*: None declared.

References

Aisa B, Gil-Bea FJ, Solas M, Garcia-Alloza M, Chen CP, Lai MK, Francis PT, Ramirez MJ. 2010. Altered NCAM expression associated with the cholinergic system in Alzheimer's disease. J Alzheimers Dis. 20:659–668.

Angata K, Long JM, Bukalo O, Lee W, Dityatev A, Wynshaw-Boris A, Schachner M, Fukuda M, Marth JD. 2004. Sialyltransferase ST8Sia-II assembles a subset of polysialic acid that directs hippocampal axonal targeting and promotes fear behavior. J Biol Chem. 279:32603–32613.

Anney R, Klei L, Pinto D, Regan R, Conroy J, Magalhaes TR, Correia C, Abrahams BS, Sykes N, Pagnamenta AT, et al. 2010. A genomewide scan for common alleles affecting risk for autism. Hum Mol Genet. 19:4072–4082.

Arai M, Yamada K, Toyota T, Obata N, Haga S, Yoshida Y, Nakamura K, Minabe Y, Ujike H, Sora I, et al. 2006. Association between polymorphisms in the promoter region of the sialyltransferase 8B (SIAT8B) gene and schizophrenia. Biol Psychiatry. 59:652–659.

Arnall S, Cheam LY, Smart C, Rengel A, Fitzgerald M, Thivierge JP, Rodger J. 2010. Abnormal strategies during visual discrimination reversal learning in ephrin-A2 (-/-) mice. Behav Brain Res. 209:109–113.

Atz ME, Rollins B, Vawter MP. 2007. NCAM1 association study of bipolar disorder and schizophrenia: polymorphisms and alternatively spliced isoforms lead to similarities and differences. Psychiatr Genet. 17:55–67.

Downloaded from https://academic.oup.com/cercor/article/23/1/162/331609 by guest on 08 August 2022

Bamji SX, Shimazu K, Kimes N, Huelsken J, Birchmeier W, Lu B, Reichardt LF. 2003. Role of beta-catenin in synaptic vesicle localization and presynaptic assembly. Neuron. 40:719–731.
Banks MI, Li TB, Pearce RA. 1998. The synaptic basis of GABAA, slow. J Neurosci. 18:1305–1317.
Barbeau D, Liang JJ, Robitalille Y, Quirion R, Srivastava LK. 1995. Decreased expression of the embryonic form of the neural cell adhesion molecule in schizophrenic brains. Proc Natl Acad Sci U S A. 92:2785–2789.
Bartos M, Vida I, Frotscher M, Meyer A, Monyer H, Geiger JR, Jonas P. 2002. Fast synaptic inhibition promotes synchronized gamma oscillations in hippocampal interneuron networks. Proc Natl Acad Sci U S A. 99:13222–13227.
Blue ME, Parnavelas JG. 1983. The formation and maturation of synapses in the visual cortex of the rat. II. Quantitative analysis. J Neurocytol. 12:697–712.
Bonfanti L. 2006. PSA-NCAM in mammalian structural plasticity and neurogenesis. Prog Neurobiol. 80:129–164.
Brennaman LH, Kochlamazashvili G, Stoenica L, Nonneman RJ, Moy SS, Schachner M, Dityatev A, Maness PF. 2011. Transgenic mice overexpressing the extracellular domain of NCAM are impaired in working memory and cortical plasticity. Neurobiol Dis. 43:372–378.
Brennaman LH, Maness PF. 2008. Developmental regulation of GABAergic interneuron branching and synaptic development in the prefrontal cortex by soluble neural cell adhesion molecule. Mol Cell Neurosci. 37:781–793.
Bukalo O, Fentrop N, Lee AY, Salmen B, Law JW, Wotjak CT, Schweizer M, Dityatev A, Schachner M. 2004. Conditional ablation of the neural cell adhesion molecule reduces precision of spatial learning, long-term potentiation, and depression in the CA1 subfield of mouse hippocampus. J Neurosci. 24:1565–1577.
Calandreau L, Marquez C, Bisaz R, Fantin M, Sandi C. 2010. Differential impact of polysialyltransferase ST8SiaII and ST8SiaIV knockout on social interaction and aggression. Genes Brain Behav. 9:958–967.
Casey JP, Magalhaes T, Conroy JM, Regan R, Shah N, Anney R, Shields DC, Abrahams BS, Almeida J, Bacchelli E, et al. Forthcoming 2011. A novel approach of homozygous haplotype sharing identifies candidate genes in autism spectrum disorder. Hum Genet.
Castellani V, Yue Y, Gao PP, Zhou R, Bolz J. 1998. Dual action of a ligand for Eph receptor tyrosine kinases on specific populations of axons during the development of cortical circuits. J Neurosci. 18:4663–4672.
Chang Y-C, Gottlieb DI. 1988. Characterization of the proteins purified with monoclonal antibodies to glutamic acid decarboxylase. J Neurosci. 8:2123–2130.
Chattopadhyaya B, Di Cristo G, Higashiyama H, Knott GW, Kuhlman SJ, Welker E, Huang ZJ. 2004. Experience and activity-dependent maturation of perisomatic GABAergic innervation in primary visual cortex during a postnatal critical period. J Neurosci. 24:9598–9611.
Chattopadhyaya B, Di Cristo G, Wu CZ, Knott G, Kuhlman S, Fu Y, Palmiter RD, Huang ZJ. 2007. GAD67-mediated GABA synthesis and signaling regulate inhibitory synaptic innervation in the visual cortex. Neuron. 54:889–903.
Ciossek T, Monschau B, Kremoser C, Loschinger J, Lang S, Muller BK, Bonhoeffer F, Drescher U. 1998. Eph receptor-ligand interactions are necessary for guidance of retinal ganglion cell axons in vitro. Eur J Neurosci. 10:1574–1580.
Close BE, Colley KJ. 1998. In vivo autopolysialylation and localization of the polysialyltransferases PST and STX. J Biol Chem. 273:34586–34593.
Colbert MC, Rubin WW, Linney E, LaMantia AS. 1995. Retinoid signaling and the generation of regional and cellular diversity in the embryonic mouse spinal cord. Dev Dyn. 204:1–12.
Colley KJ. 2010. Structural basis for the polysialylation of the neural cell adhesion molecule. Adv Exp Med Biol. 663:111–126.
Cox EC, Muller B, Bonhoeffer F. 1990. Axonal guidance in the chick visual system: posterior tectal membranes induce collapse of growth cones from the temporal retina. Neuron. 4:31–37.
Cox ET, Brennaman LH, Gable KL, Hamer RM, Glantz LA, Lamantia AS, Lieberman JA, Gilmore JH, Maness PF, Jarskog LF. 2009. Developmental regulation of neural cell adhesion molecule in human prefrontal cortex. Neuroscience. 162:96–105.
Cremer H, Chazal G, Carleton A, Goridis C, Vincent JD, Lledo PM. 1998. Long-term but not short-term plasticity at mossy fiber synapses is impaired in neural cell adhesion molecule-deficient mice. Proc Natl Acad Sci U S A. 95:13242–13247.
Cremer H, Lange R, Christoph A, Plomann M, Vopper G, Roes J, Brown R, Baldwin S, Barthels D, Rajewsky K, et al. 1994. Inactivation of the N-CAM gene in mice results in size reduction of the olfactory bulb and deficits in spatial learning. Nature. 367:455–459.
Cutforth T, Moring L, Mendelsohn M, Nemes A, Shah NM, Kim MM, Frisen J, Axel R. 2003. Axonal ephrin-As and odorant receptors: coordinate determination of the olfactory sensory map. Cell. 114:311–322.
Demyanenko GP, Siesser PF, Wright AG, Brennaman LH, Bartsch U, Schachner M, Maness PF. 2011. L1 and CHL1 cooperate in thalamocortical axon targeting. Cereb Cortex. 21:401–412.
Demyanenko GP, Tsai A, Maness PF. 1999. Abnormalities in neuronal process extension, hippocampal development, and the ventricular system of L1 knockout mice. J Neurosci. 19:4907–4920.
Depaepe V, Suarez-Gonzalez N, Dufour A, Passante L, Gorski JA, Jones KR, Ledent C, Vanderhaeghen P. 2005. Ephrin signalling controls brain size by regulating apoptosis of neural progenitors. Nature. 435:1244–1250.
Di Cristo G, Wu C, Chattopadhyaya B, Ango F, Knott G, Welker E, Svoboda K, Huang ZJ. 2004. Subcellular domain-restricted GABAergic innervation in primary visual cortex in the absence of sensory and thalamic inputs. Nat Neurosci. 7:1184–1186.
Di Cristo G, Chattopadhyaya B, Kuhlman SJ, Fu Y, Belanger MC, Wu CZ, Rutishauser U, Maffei L, Huang ZJ. 2007. Activity-dependent PSA expression regulates inhibitory maturation and onset of critical period plasticity. Nat Neurosci. 10:1569–1577.
Dityatev A, Bukalo O, Schachner M. 2008. Modulation of synaptic transmission and plasticity by cell adhesion and repulsion molecules. Neuron Glia Biol. 4:197–209.
Dityatev A, Dityateva G, Sytnyk V, Delling M, Toni N, Nikonenko I, Muller D, Schachner M. 2004. Polysialylated neural cell adhesion molecule promotes remodeling and formation of hippocampal synapses. J Neurosci. 24:9372–9382.
Dudanova I, Gatto G, Klein R. 2010. GDNF acts as a chemoattractant to support ephrinA-induced repulsion of limb motor axons. Curr Biol. 20:2150–2156.
El Maarouf A, Rutishauser U. 2003. Removal of polysialic acid induces aberrant pathways, synaptic vesicle distribution, and terminal arborization of retinotectal axons. J Comp Neurol. 460:203–211.
Esclapez M, Tillakaratne NJ, Kaufman DL, Tobin AJ, Houser CR. 1994. Comparative localization of two forms of glutamic acid decarboxylase and their mRNAs in rat brain supports the concept of functional differences between the forms. J Neurosci. 14:1834–1855.
Essrich C, Lorez M, Benson JA, Fritschy JM, Luscher B. 1998. Postsynaptic clustering of major GABAA receptor subtypes requires the gamma2 subunit and gepyhrin. Nat Neurosci. 1:563–571.
Feldblum S, Erlander MG, Tobin AJ. 1993. Different distributions of GAD65 and GAD67 mRNAs suggest that the two glutamate decarboxylases play distinctive functional roles. J Neurosci Res. 34:689–706.
Filosa A, Paixao S, Honsek SD, Carmona MA, Becker L, Feddersen B, Gaitanos L, Rudhard Y, Schoepfer R, Klopstock T, et al. 2009. Neuron-glia communication via EphA4/ephrin-A3 modulates LTP through glial glutamate transport. Nat Neurosci. 12:1285–1292.
Foldy C, Lee SY, Szabadics J, Neu A, Soltesz I. 2007. Cell type-specific gating of perisomatic inhibition by cholecystokinin. Nat Neurosci. 10:1128–1130.
Freund TF. 2003. Interneuron Diversity series: rhythm and mood in perisomatic inhibition. Trends Neurosci. 26:489–495.
Freund TF, Katona I. 2007. Perisomatic inhibition. Neuron. 56:33–42.
Galimberti I, Bednarek E, Donato F, Caroni P. 2010. EphA4 signaling in juveniles establishes topographic specificity of structural plasticity in the hippocampus. Neuron. 65:627–642.
Galuska SP, Rollenhagen M, Kaup M, Eggers K, Oltmann-Norden I, Schiff M, Hartmann M, Weinhold B, Hildebrandt H, Geyer R, et al. 2010. Synaptic cell adhesion molecule SynCAM 1 is a target for

Downloaded from https://academic.oup.com/cercor/article/23/1/162/331609 by guest on 08 August 2022

polysialylation in postnatal mouse brain. Proc Natl Acad Sci U S A. 107:10250–10255.
Gao PP, Yue Y, Zhang JH, Cerretti DP, Levitt P, Zhou R. 1998. Regulation of thalamic neurite outgrowth by the Eph ligand ephrin-A5: implications in the development of thalamocortical projections. Proc Natl Acad Sci U S A. 95:5329–5334.
Gascon E, Vutskits L, Kiss JZ. 2007. Polysialic acid-neural cell adhesion molecule in brain plasticity: from synapses to integration of new neurons. Brain Res Rev. 56:101–118.
Gomez-Climent MA, Guirado R, Castillo-Gomez E, Varea E, Gutierrez-Mecinas M, Gilabert-Juan J, Garcia-Mompo C, Vidueira S, Sanchez-Mataredona D, Hernandez S, et al. 2011. The polysialylated form of the neural cell adhesion molecule (PSA-NCAM) Is expressed in a subpopulation of mature cortical interneurons characterized by reduced structural features and connectivity. Cereb Cortex. 21:1028–1041.
Hartwich K, Pollak T, Klausberger T. 2009. Distinct firing patterns of identified basket and dendrite-targeting interneurons in the prefrontal cortex during hippocampal theta and local spindle oscillations. J Neurosci. 29:9563–9574.
Hata K, Polo-Parada L, Landmesser LT. 2007. Selective targeting of different neural cell adhesion molecule isoforms during motoneuron myotube synapse formation in culture and the switch from an immature to mature form of synaptic vesicle cycling. J Neurosci. 27:14481–14493.
Hildebrandt H, Muhlenhoff M, Gerardy-Schahn R. 2010. Polysialylation of NCAM. Adv Exp Med Biol. 663:95–109.
Hinkle CL, Diestel S, Lieberman J, Maness PF. 2006. Metalloprotease-induced ectodomain shedding of neural cell adhesion molecule (NCAM). J Neurobiol. 66:1378–1395.
Hoch RV, Rubenstein JL, Pleasure S. 2009. Genes and signaling events that establish regional patterning of the mammalian forebrain. Semin Cell Dev Biol. 20:378–386.
Isomura R, Kitajima K, Sato C. 2011. Structural and functional impairments of polysialic acid by a mutated polysialyltransferase found in schizophrenia. J Biol Chem. 286:21535–21545.
Johnson CP, Fujimoto I, Rutishauser U, Leckband DE. 2005. Direct evidence that NCAM polysialylation increases intermembrane repulsion and abrogates adhesion. J Biol Chem. 280:137–145.
Jurgenson M, Aonurm-Helm A, Zharkovsky A. 2010. Behavioral profile of mice with impaired cognition in the elevated plus-maze due to a deficiency in neural cell adhesion molecule. Pharmacol Biochem Behav. 96:461–468.
Kalus I, Bormann U, Mzoughi M, Schachner M, Kleene R. 2006. Proteolytic cleavage of the neural cell adhesion molecule by ADAM17/TACE is involved in neurite outgrowth. J Neurochem. 98:78–88.
Kim KK, Adelstein RS, Kawamoto S. 2009. Identification of neuronal nuclei (NeuN) as Fox-3, a new member of the Fox-1 gene family of splicing factors. J Biol Chem. 284:31052–31061.
Klausberger T, Magill PJ, Marton LF, Roberts JD, Cobden PM, Buzsaki G, Somogyi P. 2003. Brain-state- and cell-type-specific firing of hippocampal interneurons in vivo. Nature. 421:844–848.
Kochlamazashvili G, Senkov O, Grebenyuk S, Robinson C, Xiao MF, Stummeyer K, Gerardy-Schahn R, Engel AK, Feig L, Semyanov A, et al. 2010. Neural cell adhesion molecule-associated polysialic acid regulates synaptic plasticity and learning by restraining the signaling through GluN2B-containing NMDA receptors. J Neurosci. 30:4171–4183.
Lee MT, Chen CH, Lee CS, Chen CC, Chong MY, Ouyang WC, Chiu NY, Chuo LJ, Chen CY, Tan HK, et al. 2011. Genome-wide association study of bipolar I disorder in the Han Chinese population. Mol Psychiatry. 16:548–556.
Leshchyns'ka I, Sytnyk V, Morrow JS, Schachner M. 2003. Neural cell adhesion molecule (NCAM) association with PKCbeta2 via betal spectrin is implicated in NCAM-mediated neurite outgrowth. J Cell Biol. 161:625–639.
Lewis DA, Fish KN, Arion D, Gonzalez-Burgos G. Forthcoming 2011. Perisomatic inhibition and cortical circuit dysfunction in schizophrenia. Curr Opin Neurobiol. 21:866–872.
Linhoff MW, Lauren J, Cassidy RM, Dobie FA, Takahashi H, Nygaard HB, Airaksinen MS, Strittmatter SM, Craig AM. 2009. An unbiased expression screen for synaptogenic proteins identifies the LRRTM protein family as synaptic organizers. Neuron. 61:734–749.
Mackarehtschian K, Lau CK, Caras I, McConnell SK. 1999. Regional differences in the developing cerebral cortex revealed by ephrin-A5 expression. Cereb Cortex. 9:601–610.
Maness PF, Schachner M. 2007. Neural recognition molecules of the immunoglobulin superfamily: signaling transducers of axon guidance and neuronal migration. Nat Neurosci. 10:19–26.
Meiri KF, Saffell JL, Walsh FS, Doherty P. 1998. Neurite outgrowth stimulated by neural cell adhesion molecules requires growth-associated protein-43 (GAP-43) function and is associated with GAP-43 phosphorylation in growth cones. J Neurosci. 18: 10429–10437.
Micheva KD, Beaulieu C. 1997. Development and plasticity of the inhibitory neocortical circuitry with an emphasis on the rodent barrel field cortex: a review. Can J Physiol Pharmacol. 75:470–478.
Miller K, Kolk SM, Donoghue MJ. 2006. EphA7-ephrin-A5 signaling in mouse somatosensory cortex: developmental restriction of molecular domains and postnatal maintenance of functional compartments. J Comp Neurol. 496:627–642.
Montag-Sallaz M, Montag D, Schachner M. 2003. Altered processing of novel information in N-CAM-deficient mice. Neuroreport. 14: 1343–1346.
Muhlenhoff M, Eckhardt M, Bethe A, Frosch M, Gerardy-Schahn R. 1996. Autocatalytic polysialylation of polysialyltransferase-1. EMBO J. 15:6943–6950.
Niethammer P, Delling M, Sytnyk V, Dityatev A, Fukami K, Schachner M. 2002. Cosignaling of NCAM via lipid rafts and the FGF receptor is required for neuritogenesis. J Cell Biol. 157:521–532.
Orioli D, Henkemeyer M, Lemke G, Klein R, Pawson T. 1996. Sek4 and Nuk receptors cooperate in guidance of commissural axons and in palate formation. EMBO J. 15:6035–6049.
Pangratz-Fuehrer S, Hestrin S. 2011. Synaptogenesis of electrical and GABAergic synapses of fast-spiking inhibitory neurons in the neocortex. J Neurosci. 31:10767–10775.
Panicker AK, Buhusi M, Thelen K, Maness PF. 2003. Cellular signalling mechanisms of neural cell adhesion molecules. Front Biosci. 8:D900–D911.
Paratcha G, Ledda F, Ibanez CF. 2003. The neural cell adhesion molecule NCAM is an alternative signaling receptor for GDNF family ligands. Cell. 113:867–879.
Pfeiffenberger C, Cutforth T, Woods G, Yamada J, Renteria RC, Copenhagen DR, Flanagan JG, Feldheim DA. 2005. Ephrin-As and neural activity are required for eye-specific patterning during retinogeniculate mapping. Nat Neurosci. 8:1022–1027.
Pillai-Nair N, Panicker AK, Rodriguiz RM, Gilmore KL, Demyanenko GP, Huang JZ, Wetsel WC, Maness PF. 2005. Neural cell adhesion molecule-secreting transgenic mice display abnormalities in GABAergic interneurons and alterations in behavior. J Neurosci. 25:4659–4671.
Puchkov D, Leshchyns'ka I, Nikonenko AG, Schachner M, Sytnyk V. 2011. NCAM/Spectrin complex disassembly results in PSD perforation and postsynaptic endocytic zone formation. Cereb Cortex. 21:2217–2232.
Rey-Gallardo A, Escribano C, Delgado-Martin C, Rodriguez-Fernandez JL, Gerardy-Schahn R, Rutishauser U, Corbi AL, Vega MA. 2010. Polysialylated neuropilin-2 enhances human dendritic cell migration through the basic C-terminal region of CCL21. Glycobiology. 20:1139–1146.
Rutishauser U. 2008. Polysialic acid in the plasticity of the developing and adult vertebrate nervous system. Nat Rev Neurosci. 9:26–35.
Salaita K, Groves JT. 2010. Roles of the cytoskeleton in regulating EphA2 signals. Commun Integr Biol. 3:454–457.
Salaita K, Nair PM, Petit RS, Neve RM, Das D, Gray JW, Groves JT. 2010. Restriction of receptor movement alters cellular response: physical force sensing by EphA2. Science. 327:1380–1385.
Salin PA, Prince DA. 1996. Spontaneous GABAA receptor-mediated inhibitory currents in adult rat somatosensory cortex. J Neurophysiol. 75:1573–1588.

Downloaded from https://academic.oup.com/cercor/article/23/1/162/331609 by guest on 08 August 2022

Santuccione A, Sytnyk V, Leshchyns'ka I, Schachner M. 2005. Prion protein recruits its neuronal receptor NCAM to lipid rafts to activate p59fyn and to enhance neurite outgrowth. J Cell Biol. 169:341–354.
Schlatter MC, Buhusi M, Wright AG, Maness PF. 2008. CHL1 promotes Sema3A-induced growth cone collapse and neurite elaboration through a motif required for recruitment of ERM proteins to the plasma membrane. J Neurochem. 104:731–744.
Seki T, Rutishauser U. 1998. Removal of polysialic acid-neural cell adhesion molecule induces aberrant mossy fiber innervation and ectopic synaptogenesis in the hippocampus. J Neurosci. 18:3757–3766.
Senkov O, Sun M, Weinhold B, Gerardy-Schahn R, Schachner M, Dityatev A. 2006. Polysialylated neural cell adhesion molecule is involved in induction of long-term potentiation and memory acquisition and consolidation in a fear-conditioning paradigm. J Neurosci. 26:10888–109898.
Smith FM, Vearing C, Lackmann M, Treutlein H, Himanen J, Chen K, Saul A, Nikolov D, Boyd AW. 2004. Dissecting the EphA3/Ephrin-A5 interactions using a novel functional mutagenesis screen. J Biol Chem. 279:9522–9531.
Sohal VS, Zhang F, Yizhar O, Deisseroth K. 2009. Parvalbumin neurons and gamma rhythms enhance cortical circuit performance. Nature. 459:698–702.
Stoenica L, Senkov O, Gerardy-Schahn R, Weinhold B, Schachner M, Dityatev A. 2006. In vivo synaptic plasticity in the dentate gyrus of mice deficient in the neural cell adhesion molecule NCAM or its polysialic acid. Eur J Neurosci. 23:2255–2264.
Stork O, Welzl H, Cremer H, Schachner M. 1997. Increased intermale aggression and neuroendocrine response in mice deficient for the neural cell adhesion molecules. Eur J Neurosci. 9:424–434.
Stork O, Welzl H, Wolfer D, Schuster T, Mantei N, Stork S, Hoyer D, Lipp H, Obata K, Schachner M. 2000. Recovery of emotional behaviour in neural cell adhesion molecule (NCAM) null mutant mice through transgenic expression of NCAM180. Eur J Neurosci. 12:3291–3306.
Stork O, Welzl H, Wotjak CT, Hoyer D, Delling M, Cremer H, Schachner M. 1999. Anxiety and increased 5-HT1A receptor response in NCAM null mutant mice. J Neurobiol. 40:343–355.
Sullivan PF, Keefe RS, Lange LA, Lange EM, Stroup TS, Lieberman J, Maness PF. 2007. NCAM1 and neurocognition in schizophrenia. Biol Psychiatry. 61:902–910.
Sytnyk V, Leshchyns'ka I, Nikonenko AG, Schachner M. 2006. NCAM promotes assembly and activity-dependent remodeling of the postsynaptic signaling complex. J Cell Biol. 174:1071–1085.
Tabuchi K, Blundell J, Etherton MR, Hammer RE, Liu X, Powell CM, Sudhof TC. 2007. A neuroligin-3 mutation implicated in autism increases inhibitory synaptic transmission in mice. Science. 318:71–76.
Tao R, Li C, Zheng Y, Qin W, Zhang J, Li X, Xu Y, Shi YY, Feng G, He L. 2007. Positive association between SIAT8B and schizophrenia in the Chinese Han population. Schizophr Res. 90:108–114.
Torii M, Hashimoto-Torii K, Levitt P, Rakic P. 2009. Integration of neuronal clones in the radial cortical columns by EphA and ephrin-A signalling. Nature. 461:524–528.
Tran TS, Rubio ME, Clem RL, Johnson D, Case L, Tessier-Lavigne M, Huganir RL, Ginty DD, Kolodkin AL. 2009. Secreted semaphorins control spine distribution and morphogenesis in the postnatal CNS. Nature. 462:1065–1069.
Vaidya A, Pniak A, Lemke G, Brown A. 2003. EphA3 null mutants do not demonstrate motor axon guidance defects. Mol Cell Biol. 23:8092–8098.
van Kammen DP, Poltorak M, Kelley ME, Yao JK, Gurklis JA, Peters JL, Hemperly JJ, Wright RD, Freed WJ. 1998. Further studies of elevated cerebrospinal fluid neuronal cell adhesion molecule in schizophrenia. Biol Psychiatry. 43:680–686.
Vawter MP. 2000. Dysregulation of the neural cell adhesion molecule and neuropsychiatric disorders. Eur J Pharmacol. 405:385–395.
Vawter MP, Usen N, Thatcher L, Ladenheim B, Zhang P, VanderPutten DM, Conant K, Herman MM, van Kammen DP, Sedvall G, et al. 2001. Characterization of human cleaved N-CAM and association with schizophrenia. Exp Neurol. 172:29–46.
Waagepetersen HS, Qu H, Hertz L, Sonnewald U, Schousboe A. 2002. Demonstration of pyruvate recycling in primary cultures of neocortical astrocytes but not in neurons. Neurochem Res. 27:1431–1437.
Weinhold B, Seidenfaden R, Rockle I, Muhlenhoff M, Schertzinger F, Conzelmann S, Marth JD, Gerardy-Schahn R, Hildebrandt H. 2005. Genetic ablation of polysialic acid causes severe neurodevelopmental defects rescued by deletion of the neural cell adhesion molecule. J Biol Chem. 280:42971–42977.
White JA, Banks MI, Pearce RA, Kopell NJ. 2000. Networks of interneurons with fast and slow gamma-aminobutyric acid type A (GABAA) kinetics provide substrate for mixed gamma-theta rhythm. Proc Natl Acad Sci U S A. 97:8128–8133.
Whittington MA, Traub RD. 2003. Interneuron diversity series: inhibitory interneurons and network oscillations in vitro. Trends Neurosci. 26:676–682.
Williams SR, Mitchell SJ. 2008. Direct measurement of somatic voltage clamp errors in central neurons. Nat Neurosci. 11:790–798.
Wong EV, Kerner JA, Jay DG. 2004. Convergent and divergent signaling mechanisms of growth cone collapse by ephrinA5 and slit2. J Neurobiol. 59:66–81.
Wright AG, Demyanenko GP, Powell A, Schachner M, Enriquez-Barreto L, Tran TS, Polleux F, Maness PF. 2007. Close homolog of L1 and neuropilin 1 mediate guidance of thalamocortical axons at the ventral telencephalon. J Neurosci. 27:13667–13679.
Xu X, Roby KD, Callaway EM. 2010. Immunochemical characterization of inhibitory mouse cortical neurons: three chemically distinct classes of inhibitory cells. J Comp Neurol. 518:389–404.
Yun ME, Johnson RR, Antic A, Donoghue MJ. 2003. EphA family gene expression in the developing mouse neocortex: regional patterns reveal intrinsic programs and extrinsic influence. J Comp Neurol. 456:203–216.

Downloaded from https://academic.oup.com/cercor/article/23/1/162/331609 by guest on 08 August 2022